

1 Environmental and biological controls on Na/Ca ratios in
2 scleractinian cold-water corals

3 Nicolai Schleinkofer^{1,2}, Jacek Raddatz^{1,2}, André Freiwald^{3,4}, David Evans^{1,2}, Lydia Beuck³,
4 Andres Rüggeberg⁴, Volker Liebetrau⁵

5 ¹Institute of Geosciences, Goethe University Frankfurt, Altenhöferallee 1, 60438 Frankfurt am Main,
6 Germany

7 ²Frankfurt Isotope and Element Research Center (FIERCE), Goethe University Frankfurt,
8 Altenhöferallee 1, 60438 Frankfurt am Main, Germany

9 ³Senckenberg am Meer, Marine Research Department, Südstrand 40, 26382 Wilhelmshaven,
10 Germany

11 ⁴MARUM (Zentrum für Marine Umweltwissenschaften), Bremen University, Leobener Str. 8,
12 28359 Bremen, Germany

13 ⁵Department of Geosciences, Faculty of Science and Medicine, University of Fribourg, Chemin du
14 Musée 6, CH-1700 Fribourg, Switzerland

15 ⁶GEOMAR Helmholtz Centre for Ocean Research Kiel, Wischhofstr. 1-3, D-24148 Kiel, Germany

16

17 Correspondence to: Nicolai Schleinkofer (schleinkofer@em.uni-frankfurt.de)

18

19 **Abstract**

20 Here we present a comprehensive attempt to correlate aragonitic Na/Ca ratios from
21 *Desmophyllum pertusum* (formerly known as *Lophelia pertusa*), *Madrepora oculata* and a
22 caryophylliid cold-water coral (CWC) species with different seawater parameters such as
23 temperature, salinity and pH. Living CWC specimens were collected from 16 different locations
24 and analyzed for their Na/Ca ratios using solution-based inductively coupled plasma-optical
25 emission spectrometry (ICP-OES) measurements.

26 The results reveal no apparent correlation with salinity (30.1–40.57 g/kg), but a significant
27 inverse correlation with temperature (-0.31 ± 0.04 mmol/mol/°C). Other marine aragonitic
28 organisms such as *Mytilus edulis* (inner aragonitic shell portion) and *Porites* sp. exhibit similar
29 results highlighting the consistency of the calculated CWC regressions. Corresponding Na/Mg
30 ratios show a similar temperature sensitivity to Na/Ca ratios, but the combination of two ratios
31 appear to reduce the impact of vital effects and domain-dependent geochemical variation. The
32 high degree of scatter and elemental heterogeneities between the different skeletal features in
33 both Na/Ca and Na/Mg however limit the use of these ratios as a proxy and/or make a high
34 number of samples necessary. Additionally, we explore two models to explain the observed
35 temperature sensitivity of Na/Ca ratios for an open and semi-enclosed calcifying space based
36 on temperature sensitive Na and Ca pumping enzymes and transport proteins that change the
37 composition of the calcifying fluid and consequently the skeletal Na/Ca ratio.

38 **1. Introduction**

39 Sodium to calcium ratios (Na/Ca) has been proposed as a new tool in paleoceanography to
40 reconstruct seawater salinities. Cultured benthic and planktonic foraminifera as well as living
41 planktonic foraminifera from the Red Sea showed the potential of calcitic Na/Ca ratios as an
42 salinity proxy (Mezger et al., 2016; Wit et al., 2013). Cold-water corals provide one of the most
43 promising marine paleoenvironmental archives for climatic research due to the potential to
44 reconstruct high-resolution records using the aragonitic skeleton (Druffel, 1997). About half of
45 the known scleractinian coral species do not live in tropical, shallow water (<50 m) but in

46 deeper waters, including deep-sea environments (>200 m) (Roberts et al., 2009). These deep
47 or cold-water corals lack phototrophic symbionts and therefore are azooxanthellate. Like their
48 zooxanthellate shallow-water relatives, some azooxanthellate deep water species, such as
49 *Desmophyllum pertusum* and *Madrepora oculata*, are also capable of building large three-
50 dimensional reef frameworks that serve as habitats for thousands of different organisms and
51 constitute biodiversity hotspots in low to high latitudes and from shallower water to the deep
52 seas (Henry and Roberts, 2016; Roberts et al., 2009). The distribution of CWC is controlled by
53 several parameters, amongst which is the density of seawater (Dullo et al., 2008) which
54 appears to correlate with the so called Intermediate Nepheloid Layers (INL). These INL
55 contribute an important source of particulate organic matter (POM) (Kiriakoulakis et al., 2005,
56 2007) that CWC feed on. Additionally, it has been suggested, that gamete density restricts the
57 lateral transport to certain density envelopes (Dullo et al., 2008). For *D. pertusum*, the suitable
58 density envelope amounts to $\sigma_{\theta} = 27.35\text{--}27.65 \text{ kg/m}^3$ (Dullo et al., 2008), although these
59 values are not applicable to every oceanic region (Flögel et al., 2014; Freiwald et al., 2009;
60 Rüggeberg et al., 2011). Since seawater density is a function of temperature and salinity, these
61 parameters also partly control the spatial distribution of CWC. Most known CWC occur in
62 salinities of 35 g/kg and mean temperatures of 4–12°C (Freiwald, 2002; Freiwald and Roberts,
63 2005), although they are also able to thrive in lower and higher temperatures and salinities
64 (e.g. Bett, 2001; Roder et al., 2013; Taviani et al., 2005).

65 Independent proxies are needed to reconstruct the environment in which CWC lived in the past
66 to better understand their temperature/salinity/pH tolerances and to study the influence of
67 parameters on their spatial distribution. This would also help to better locate new unknown
68 sites of CWC occurrences. For temperature and pH, different geochemical proxies can be used
69 to calculate these parameters in the geological past. Sr/Ca and Li/Mg ratios serve as
70 temperature proxies (Cohen et al., 2006; Gagnon et al., 2007; Mitsuguchi et al., 1996;
71 Montagna et al., 2014; Raddatz et al., 2013, 2014a; Rollion-Bard and Blamart, 2015; Shirai et
72 al., 2005), U/Ca and Boron-isotopes serve as proxies of the carbonate system (Anagnostou et
73 al., 2011, 2012; Blamart et al., 2007; McCulloch et al., 2012; Raddatz et al., 2014b, 2016;

74 Rollion-Bard et al., 2011). However, independent geochemical methods to reconstruct past
75 salinities are absent but urgently needed to reconstruct spatial distribution patterns in the past
76 and quantify effects of ocean acidification on CWC by researching its effects in the past. Even
77 though CWC show that they can maintain growth in under-saturated, corrosive waters, the
78 older unprotected parts of the reef are susceptible for dissolution (Büscher et al., 2017; Form
79 and Riebesell, 2012). This weakens the reef integrity and might cause severe implications on
80 available microhabitats (Büscher et al., 2017; Roberts, 2006)

81 Reconstructing past salinities can be accomplished with several different techniques, e.g.
82 diatom and dinoflagellate species composition (Zonneveld et al., 2001), morphology and size
83 of placoliths from *Emiliana huxleyi* (Bollmann et al., 2009), Ba/Ca ratios in foraminiferal calcite
84 (Weldeab et al., 2007), the strontium isotope composition of bivalves (Israelson and Buchardt,
85 1999), process length of dinoflagellate cysts (Mertens et al., 2009), hydrogen isotope
86 composition of alkenones (van der Meer et al., 2007; Schouten et al., 2006) or temperature
87 corrected (Mg/Ca, TEX₈₆) oxygen isotopes (Elderfield and Ganssen, 2000). While some of
88 these proxies may yield reliable results (e.g. coupled Mg/Ca and oxygen isotopes (Elderfield
89 et al., 2012; Lear et al., 2000)) others suffer from rather large uncertainties introduced by
90 modelled parameters or require a good knowledge of the regional oceanography (Wit et al.,
91 2013). Others, like Ba/Ca ratios are more effected by terrestrial runoff and are therefore only
92 applicable in proximal sites. Complications with the existing proxies mean that further methods
93 are desirable, therefore we explore here whether coral Na/Ca ratios may be useful in this
94 regard.

95 The influence of seawater salinity on Na/Ca ratios are known from Atlantic oysters (Rucker
96 and Valentine, 1961), barnacle shells (Gordon et al., 1970) as well as inorganically precipitated
97 calcium carbonate (Ishikawa and Ichikuni, 1984). Recently it has been shown that Na
98 incorporation in calcitic planktonic and benthic foraminifera **appears to be at least partly**
99 **controlled** by seawater salinity (Allen et al., 2016 (only in *Globigerinoides ruber*); Mezger et al.,
100 2016; Wit et al., 2013). According to Wit et al. (2013), the incorporation of Na in calcite depends

101 on the activity of Na in the seawater which is a function of salinity. There is strong evidence
102 that Na substitutes for Ca in biogenic aragonite despite its charge difference (Okumura and
103 Kitano, 1986; Yoshimura et al., 2017). However, since Na and Ca compete for the same lattice
104 positions, the calcium concentration and Na/Ca activity ratio of the surrounding seawater might
105 also control the amount of sodium incorporation (Ishikawa and Ichikuni, 1984; White, 1977).
106 Over longer periods of geological time, when concentrations of some elements in seawater
107 have varied, this would inhibit the use of Na/Ca ratios as a salinity proxy but might prove useful
108 to reconstruct oceanic calcium concentrations. Recent studies also show that the Na/Ca ratio
109 in foraminiferal calcite is also mainly controlled by seawater Na/Ca ratios (Hauzer et al., 2018).
110 In this study, we investigate the impact of different seawater parameters on the incorporation
111 of Na in the aragonitic skeleton of the scleractinian cold-water coral *D. pertusum*, *M. oculata*
112 and a caryophylliid species from the Red Sea. The corals were collected alive from a variety
113 of locations to cover a broad range of temperatures (5.9–21.6°C) and salinities (30.1–40.6
114 g/kg).

115 **2. Materials & Methods**

116 **2.1. Study area and sample collection**

117 The samples were taken from 45 different coral specimens collected from 16 different locations
118 (Tab. 1). Most of the samples (n=25) were collected during different cruises from the
119 Norwegian margin. The other samples derive from the Irish Margin and Bay of Biscay (n=4),
120 the Mediterranean Sea and Gulf of Cadiz (n=7), the Gulf of Mexico and Great Bahama Bank
121 (n=4) and the Red Sea (n=5) (Fig. 1). Conductivity-Temperature-Depth (CTD) downcast data
122 for water parameters was available for all locations except the Red Sea and the Gulf of Mexico.
123 Where no CTD data was available, the water parameters were retrieved from annual averaged
124 data from World Ocean Atlas 2013 (Locarnini et al., 2013; Zweng et al., 2013). Where
125 available, comparison of *in-situ* CTD and WOA13 data, revealed an agreement within 0.15°C
126 in Santa Maria de Leuca and 0.04°C in the Bay of Biscay respectively. **The seawater carbonate
127 system data such as pH was taken from the associated cruise report (Flögel et al., 2014) or in**

128 case of the Red Sea and the western Atlantic from Mezger et al., (2016) and CARINA. Flögel
129 et al., 2014 used a WTW Multi 350i compact precision hand- held meter to determine pH
130 (Flögel et al., 2014), pH in the Red Sea was calculated from DIC and TA, measured during
131 PELAGIA 64PE158 (Mezger et al., 2016), using CO2SYS (Lewis and Wallace, 1998). pH
132 values are reported using the total scale.

133 We took 31 samples from different coral colonies and three different species (*D. pertusum*, *M.*
134 *oculata*, Caryophylliidae) that were collected during different cruises. The samples were taken
135 from the uppermost calices after physically cleaning them with a dental drill tool to remove
136 secondary overgrowths. We avoided further cleaning or rinsing with water because studies
137 suggest that structurally substituted Na is readily leached even by distilled water (Ragland et
138 al., 1979). It is possible that organic contents inside the skeleton bias the results **as shown in**
139 **foraminifera** (Branson et al., 2016). However, the study on foraminifera shows that the Na/Ca
140 ratio only significantly varies at POS (primary organic sheet) regions. In corals the COC
141 (centers of calcification) would be an equivalent structure, which we avoided during the
142 sampling process. Furthermore, it has been suggested that these regions only significantly
143 affect bulk sample elemental ratios in very thin-walled foraminifera (Branson et al., 2016). In
144 corals the area of COC is larger (20% of the total skeleton radius (Rollion-Bard and Blamart,
145 2015)) but the Na/Ca ratio does not increase in the COC as strong as it does in the POS areas
146 of foraminifera (Branson et al., 2016; Rollion-Bard and Blamart, 2015). Avoiding the COC areas
147 in bulk samples only reduces the mean Na/Ca ratio by 0.18 mmol/mol (**0.18 mmol/mol =**
148 **$\overline{Na/Ca}_{inc. COC}^{Sample 1-i} - \overline{Na/Ca}_{exc. COC}^{Sample 1-i}$**), additional cleaning of organic material is therefore not
149 necessary. An additional 14 samples (*D. pertusum*) were prepared as longitudinal slices
150 through the coral's calice, glued on metal plates. In order to identify elemental heterogenities
151 within the theca wall, subsamples were taken using a micromill (Merchantec MM-000-134).

152 **2.2. ICP-OES Analyses**

153 Elemental ratios were measured by inductively coupled plasma optical emission spectrometry
154 (ICP-OES). The ICP-OES analysis was carried out with a ThermoScientific iCap 6300 dual

155 viewing at Goethe University/Frankfurt. This machine is both capable of measuring axially and
156 radially. Alkali metals (Na) were measured radially on line 589.59 nm whereas earth-alkali
157 metals (Mg, Sr) were measured axially on lines 279.55 nm and 421.55 nm respectively. The
158 sample powder ($\approx 140 \mu\text{g}$) was dissolved in 500 μl HNO_3 (2%) and 300 μl aliquots were
159 separated. Subsequently 1500 μl of 1.2 mg/l yttrium solution was added to each aliquot as an
160 internal standard resulting in 1 mg/l. The intensity data was background subtracted and
161 standardized internally to Y and normalized to Ca. External standards were mixed from single
162 element standard solutions to match the typical element concentrations of cold-water corals
163 (cf. Rosenthal et al., 1988). The coral standard JCp-1 (Hathorne et al., 2013; Okai et al., 2002)
164 was measured after every tenth sample to allow for drift correction and monitor measurement
165 quality.

166 Relative precision of the Element/Ca measurements was based on the international calcium-
167 carbonate standard JCp-1 (20 replicates) and amounts to 20.47 ± 0.68 mmol/mol Na/Ca (19.8
168 ± 0.14 mmol/mol (Okai et al., 2002)), 4.09 ± 0.11 mmol/mol Mg/Ca (4.199 ± 0.065 mmol/mol
169 (Hathorne et al., 2013; Okai et al., 2002)) and 9.36 ± 0.07 mmol/mol Sr/Ca (8.838 ± 0.042
170 mmol/mol (Hathorne et al., 2013; Okai et al., 2002)). Measurements were conducted in two
171 sessions lasting ten and five hours.

172 **2.3. Data Processing**

173 Before calculations of correlations or applying statistics outliers were removed from the raw
174 data. Outliers were identified by the average ± 1.5 SD per oceanic region (Norwegian margin,
175 Bay of Biscay/Irish Margin, Mediterranean Sea, Red Sea, Gulf of Mexico/Bahamas). The
176 threshold was chosen to eliminate data points <15 mmol/mol and >35 mmol/mol cover a range
177 from 15 to 35 mmol/mol which is roughly 5 mmol/mol higher and lower than the reported range
178 from a similar study (Rollion-Bard and Blamart, 2015). The profiled samples were additionally
179 checked for values that derive from the COC, which are identifiable through a positively
180 correlating increase in Mg/Ca and Na/Ca. The chosen threshold was the mean of the profiled

181 sample + 2SD of JCp-1. Statistical calculations were conducted with the ORIGIN Pro software
182 suite.

183 3. Results

184 Spatial distribution patterns show great variations in Na/Ca ratios through the corals skeleton
185 (Fig. 2). In the COC and COC-like structures (structures that geochemically correspond to
186 COC but morphologically to fibrous deposits) Na/Ca ratios show significant increases but the
187 amount of increase relative to the mean is not uniform in the sample. Increases range from +2
188 to +10 mmol/mol. Mg/Ca is positively correlated with Na/Ca in the COC structures but mostly
189 independent from each other in the fibrous deposits (FD). Similar to Na/Ca, the amplitude of
190 Mg/Ca in the COC-structures is very variable in their amount and ranges from +0.5 to +3
191 mmol/mol. Both sodium and magnesium are often enriched in the outermost parts of the theca.
192 Sr/Ca ratios are mostly stable throughout the theca and seem to be independent from the
193 different skeletal structures. In some samples, co-variances between Sr/Ca and Mg/Ca;Na/Ca
194 are present but in general they do not appear to be controlled by the skeletal morphology in
195 the same way as Mg/Ca and Na/Ca as shown by their independency from the different skeletal
196 structures.

197 3.1 Element/Ca ratios of scleractinian cold-water corals

198 Na/Ca ratios vary between 20.49 ± 1.36 (1SD) mmol/mol in the Red Sea and 31.04 ± 1.36
199 mmol/mol in the Norwegian reefs with a mean at 25.22 mmol/mol and a standard deviation of
200 2.8 mmol/mol (Fig. 3). The values are in accordance to previous studies on *D. pertusum*
201 (21.94–28.11 mmol/mol (Rollion-Bard and Blamart, 2015)), but 5 mmol/mol higher than
202 reported for zooxanthellate corals (Amiel et al., 1973; Busenberg and Niel Plummer, 1985;
203 Mitsuguchi et al., 2001; Ramos et al., 2004; Swart, 1981). Significant deviations between *D.*
204 *pertusum* ($n=38$), *M. oculata* ($n=2$) and Caryophylliidae ($n=5$) are not observable. A linear
205 correlation between salinity and Na/Ca over the whole salinity range is not observable, but the
206 present dataset is best described with a second order polynomial function. Accordingly, there
207 is a positive trend from 30.1–35 g/kg followed by a negative trend from 35–40.5 g/kg. Linear

208 regressions equal: $f(S_{30.1-35}) = 6.4 + 0.56 * S$ ($R^2 = 0.99, P = 0.072$) and $f(S_{35-40.5}) = 56.61 -$
 209 $0.84 * S$ ($R^2 = 0.66, P = 0.4$). As the P -values show a significant slope is missing in all these
 210 regressions. In the case of the polynomial fit the P -value shows that the fit is not significantly
 211 superior to $f(S_{30.1-40.5}) = \text{constant}$.

212 Na/Ca and temperature show a significant negative correlation, which is however mainly driven
 213 by the samples from the highest temperature (Red Sea). The linear regression equals:

$$214 \quad f_{T_{6-22^\circ\text{C}}} = 28.2 \pm 0.9 - 0.31 \pm 0.07 \times T \quad (R^2 = 0.87, P = 0.02) \quad (1)$$

215 Temperature and salinity show a positive correlation, accordingly this negative correlation
 216 cannot be caused by covariances between salinity and temperature. Corals from the
 217 Mediterranean Sea are slightly elevated in their Na/Ca ratio, but within error they still fit the
 218 correlation with both salinity and temperature. Distribution coefficients ($K_d^{\text{Na}} = \text{Na}/\text{Ca}_{\text{carbonate}}/$
 219 $\text{Na}/\text{Ca}_{\text{seawater}}$) at specific temperatures for several different species, including the scleractinian
 220 cold-water corals from this study, *Porites* sp. and *M. edulis*, show similar values. K_d^{Na} from this
 221 study amounts to $K_d^{\text{Na}}(6.2^\circ\text{C}) = 5.73 * 10^{-4}$, $K_d^{\text{Na}}(7.9^\circ\text{C}) = 5.51 * 10^{-4}$, $K_d^{\text{Na}}(9.8^\circ\text{C}) = 5.44 * 10^{-4}$, $K_d^{\text{Na}}(13.5^\circ\text{C})$
 222 $= 5.62 * 10^{-4}$, $K_d^{\text{Na}}(21.6^\circ\text{C}) = 4.73 * 10^{-4}$. Distribution coefficients for *Porites* sp. and *M. edulis* are
 223 $K_d^{\text{Na}}(26.03^\circ\text{C}) = 4.6 * 10^{-4}$ (Mitsuguchi et al., 2001) and $K_d^{\text{Na}}(12.5^\circ\text{C}) = 5.25 * 10^{-4}$ (Lorens and Bender,
 224 1980) respectively. For comparison, the inorganic distribution coefficient is with $4.00 * 10^{-4}$ at
 225 15°C , about 20% lower (Kinsman, 1970). The results from White (1977) show that the
 226 composition of the solution affects the elemental ratios in the precipitate, but in the study from
 227 Kinsman (1970) the precipitation happened from seawater. Therefore, it is reasonable to use
 228 this data for comparison. A combined regression using the data from this study, the *D.*
 229 *pertusum* data from Rollion-Bard and Blamart (2015), *M. edulis* data from Lorens and Bender
 230 (1980) and *Porites* sp. data from Ramos et al. (2004) and Mitsuguchi et al. (2001) equals:

$$231 \quad f_{T_{6-27.63^\circ\text{C}}} = 28.03 \pm 0.7 - 0.31 \pm 0.04 \times T \quad (R^2 = 0.9, P < 0.0001) \quad (2).$$

232 Na/Ca also shows a significant positive correlation with pH of the ambient seawater. Linear
233 regression equals: $f(\text{pH}) = -84.26 \pm 40.15 + 13.63 \pm 5.49 * \text{pH}$ ($R^2 = 0.14$, $P = 0.017$). A negative
234 trend between pH and temperature is visible.

235 3.2. Mg/Ca & Sr/Ca

236 Mg/Ca values vary between 2.2 ± 0.2 mmol/mol in the Red Sea and 6.38 ± 0.2 mmol/mol in
237 the Mediterranean Sea with a mean of 3.99 mmol/mol and a standard deviation of 0.97
238 mmol/mol (Fig. 4). Maximum values are higher than literature states for *D. pertusum* (2.99–
239 4.72 mmol/mol (Cohen et al., 2006; Gagnon et al., 2007; Raddatz et al., 2013; Rollion-Bard
240 and Blamart, 2015)) but the mean values are well inside the range of literature. Significant
241 deviations between *D. pertusum*, *M. oculata* and Caryophylliidae are not observable, although
242 there are limited published data *M. oculata* and Caryophylliidae. Seawater parameters such
243 as temperature, salinity and pH have no significant effect on Mg/Ca ratios in the skeleton.

244 Sr/Ca values vary between 9.46 ± 0.14 and 10.46 ± 0.14 mmol/mol with a mean of 10.1 ± 0.14
245 mmol/mol and a standard deviation of 0.25 mmol/mol (Fig. 5). Both maximum and minimum
246 values derive from corals that grew in reefs that are located in the Trondheimfjord. The values
247 are in accordance to previous studies on *D. pertusum* (9.27–10.05 mmol /mol (Cohen et al.,
248 2006; Gagnon et al., 2007; Raddatz et al., 2013)). Significant deviations between *D. pertusum*,
249 *M. oculata* and Caryophylliidae are not observable. Despite the known temperature effect on
250 Sr/Ca ratios this effect is not pronounced in this dataset. The correlation shows a strongly
251 deviating slope of -0.015 mmol/mol/°C in comparison to that given in literature (-0.083 ± 0.017
252 mmol/mol/°C (Raddatz et al., 2013)). Linear regressions equal: $f(T) = 10.26 \pm 0.05 - 0.015 \pm$
253 $0.004 * T$ ($R^2 = 0.83$, $P = 0.03$). Sr/Ca vs. salinity values show a distribution pattern similar to
254 that of Na/Ca vs. salinity values with the maximum at 35 g/kg and descending values at lower
255 and higher salinities but an AIC and a F-Test confirm that a linear fit is better suited. The Linear
256 regression equals $f(S) = 10.58 \pm 0.03 - 0.015 \pm 0.01 * S$ ($R^2 = 0.52$, $P = 0.17$). *P*-values show
257 that the correlation is not significant.

258 3.3 Element concentrations in the extracellular calcifying fluid (ECF)

259 Based on the assumption of a semi-enclosed ECF with seawater-leakage and a consequent
 260 $[Na]_{ECF}$ similar to $[Na]_{Seawater}$ it is possible to calculate $[Ca]_{ECF}$ and $[Mg]_{ECF}$ using skeletal Na/Ca
 261 and Mg/Ca data. Assuming $[Na]_{Seawater} = [Na]_{ECF} = 455$ mmol/l (Turekian et al., 2010) and an
 262 invariant Na distribution coefficient, $[Ca]_{ECF}$ can be calculated with the following equation:

$$263 \quad [Ca]_{ECF} = [Na]_{ECF} * \frac{K_d^{Na}}{\frac{Ca_{Coral}}{Na}} \quad (3)$$

264 In order to do so, knowledge of K_d^{Na} is required. White (1977) reports $1.8 - 4.1 * 10^{-4}$ for inorganic
 265 aragonite in the four experiments with solution Na/Ca closest to the natural seawater ratio (~45
 266 mol/mol), which would result in predicted aragonite Na/Ca ratios of 8 – 18 mmol/mol, slightly
 267 lower than the coral aragonite values we measure. Because this difference may be explained
 268 via differences in (e.g.) inorganic and coral aragonite growth rates (Mucci, 1988; White, 1977;
 269 Yoshimura et al., 2017) or the presence of organics (Amiel et al., 1973; Cuif et al., 2003;
 270 Stolarski, 2003), we adjust our data so that the predicted aragonite Na/Ca ratios fit our
 271 measured ratios by using $K_d^{Na} = 5.37 * 10^{-4}$ calculated from the coral samples presented here.
 272 As such we cannot presently constrain absolute $[Ca]_{ECF}$ values using this method, however the
 273 aim here is simply to explore whether differences in $[Ca]_{ECF}$ can explain the variance in both
 274 our Na/Ca and Mg/Ca data. An improved understanding of the inorganic distribution coefficient
 275 may enable both precise and accurate ECF reconstructions in the future. Using the method
 276 outlined above, we calculate $[Ca]_{ECF}$ values ranging from 7.9 mmol/l to 12.3 mmol/l with a mean
 277 of 9.9 mmol/l. This range is in good agreement with the microsensor studies on *Galaxea*
 278 *fascicularis* conducted by Al-Horani et al., (2003)(9-11 mmol/l). By substituting these data into
 279 the equation:

$$280 \quad [Mg]_{ECF} = \frac{Mg}{Ca_{Coral}} * \frac{[Ca]_{ECF}}{K_d^{Mg}} \quad (4)$$

281 With $K_d^{Mg} = 7.9 * 10^{-4}$, calculated from the coral samples presented here, $[Mg]_{ECF}$ can also be
 282 calculated. Resulting values range from 32.8 mmol/l to 104.7 mmol/l and a mean of 51.5 mmol/l
 283 and a median of 46.5 mmol/l. Results show that the Mg-concentration in the ECF is constant
 284 with changing Ca-concentration.

285 **4. Discussion**

286 **4.1 Heterogeneities of elemental ratios in scleractinian corals**

287 Ninety percent of the sodium in corals is located in the aragonitic mineral phase, the remaining
288 sodium is bound to organic material and exchangeable sites (Amiel et al., 1973). Magnesium,
289 which co-varies with sodium, is not located in the aragonitic phase but either organic material
290 (20–30%) and a highly disordered inorganic phase such as amorphous calcium carbonate
291 (ACC) (70–80%) (Amiel et al., 1973; Finch and Allison, 2008) or nanodomains of Mg-bearing
292 carbonate occluded in the aragonite (Finch and Allison, 2008). A small percentage seems to
293 be also trapped along the (001) surface (Ruiz-Hernandez et al., 2012). Elemental
294 heterogeneities are particularly visible when comparing COC and fibrous deposits (Fig. 2).
295 COC are both chemically and morphologically distinct from the fibrous deposits. While the
296 COC are built by sub-micron sized granular crystals (Constantz, 1989), the fibers that build the
297 fibrous zones are not single orthorhombic crystals but elongated composite structures with
298 very fine organo-mineral alternations (Cuif and Dauphin, 1998). Reasons for the different
299 chemical composition are still under debate and include: (1) pH variations in the calcifying fluid
300 (Adkins et al., 2003; Holcomb et al., 2009), (2) Rayleigh fractionation (Cohen et al., 2006;
301 Gagnon et al., 2007), (3) kinetic fractionation (McConnaughey, 1989; Sinclair et al., 2006), (4)
302 mixed ion transport through direct seawater transport and ionic pumping (Gagnon et al., 2012),
303 and (5) precipitation from different compartments (Meibom et al., 2004; Rollion-Bard et al.,
304 2010, 2011).

305 The missing co-variance between Sr/Ca and Mg/Ca or Na/Ca ratios excludes Rayleigh
306 fractionation as the main mechanism responsible for the large variances of elemental ratios
307 (Rollion-Bard and Blamart, 2015), as well as mixed ion transport for similar reasons (Rollion-
308 Bard and Blamart, 2015). pH variations and consequent changes in the saturation of the
309 calcifying fluid have been shown to alter Mg/Ca ratios in corals and abiogenic aragonite
310 (Holcomb et al., 2009) and therefore, could potentially alter Na/Ca ratios as well. While the pH-
311 elevation at the COC is supported by several studies (McCulloch et al., 2012; Raddatz et al.,

2014b; Sinclair et al., 2006), Tambutté et al. (2007) propose that the nanometer-sized spaces between the skeleton and the calicoblastic ectoderm does not allow a modification of the saturation state. Also, studies based on $\delta^{11}\text{B}$ measurements show that the COC might be an area of lower pH-values compared to the fibrous zones (Blamart et al., 2007; Jurikova et al., 2019; Rollion-Bard et al., 2011). Our data may be explained by different calcification compartments (Meibom et al., 2004; Rollion-Bard et al., 2010, 2011) in combination with kinetic effects caused by rapid calcification rates. Additionally, we propose changing organic contents as a further mechanism that controls elemental ratio differences in the different skeletal parts, visible in the covariance of Mg/Ca and Na/Ca ratios throughout the skeleton. However, it is not clear in what way the different precipitation regions are distinct from each other, for example whether they are characterized by different cell types or different modes of the same cell types (Rollion-Bard et al., 2010). So far, only calicoblasts and desmocytes are known from the aboral ectoderm of corals (Allemand et al., 2011; Tambutté et al., 2007) but calicoblasts show differences in their morphology, ranging from very thin, long and flat to thick and cup like (Tambutté et al., 2007). A major controlling factor on the cell shape is the calcification activity, with flat calicoblasts corresponding to low calcification activity and thick calicoblasts to high calcification activity (Tambutté et al., 2007). These different cell morphologies might be the reason for different types of precipitation, ACC, a proposed precursor phase of aragonite (Von Euw et al., 2017; Rollion-Bard et al., 2010), and granular crystals in the COC regions or organo-mineral fibers in the fibrous deposits. The precipitation of ACC in the COC would certainly explain the enrichment of Mg in these areas, as it is necessary to stabilize the otherwise unstable ACC (Von Euw et al., 2017), however, the relevance of ACC to coral calcification has been questioned as it has so far not been possible to form ACC under carbonate system conditions thought to characterize the calcification space (Evans et al., 2019). Alternatively, the COC are known to be rich in organic material (Cuif et al., 2003; Stolarski, 2003), which would also explain the enrichment of Mg as well as explaining a slight enrichment of Na. However, the amount of Na bound to organic material is not high enough (Amiel et al., 1973) that the enrichment in the COC can be solely explained by high organic contents. Kinetic

340 effects, due to rapid calcification rates are more likely to be the main control for Na variations
341 in COC and fibrous deposits. Since Na is incorporated in the aragonite lattice by direct
342 substitution with Ca (Okumura and Kitano, 1986; Yoshimura et al., 2017), charge differences
343 occur due to the exchange of divalent Ca with monovalent Na. These charge differences need
344 to be compensated by lattice defects (CO_3^{2-} vacancies), which occur more often at higher
345 precipitation rates (Mucci, 1988; White, 1977; Yoshimura et al., 2017). Growth rate effects are
346 also known for the incorporation of Mg into inorganic aragonite, albeit these effects more likely
347 result from crystal surface entrapment of Mg by new formed aragonite (Gabitov et al., 2008,
348 2011; Watson, 1996).

349 Sr/Ca ratios in the warm-water coral *Pocillopora damicornis* seems to be largely unaffected by
350 growth rate changes over a range of one to over 50 $\mu\text{m}/\text{day}$ (Brahmi et al., 2012), at least when
351 comparing different skeletal architectures (Fig. 2). This is supported by our data as the
352 observed Sr/Ca ratios show no significant decrease in the COC or COC-like areas as would
353 be expected from the results of de Villiers et al. (1994) despite the significantly different growth
354 rates in these areas (COC > 50–60 $\mu\text{m}/\text{day}$, FD = 1–3 $\mu\text{m}/\text{day}$ (Brahmi et al., 2012)). In fact,
355 an increase in the COC is more often but still not regularly visible (Cohen et al., 2006).
356 Consequently, a significant effect of the different skeletal architectures on Sr/Ca ratios in
357 coralline aragonite can be excluded. Slight increases in the COC however can be explained
358 with the great adsorption potential of Sr to organic matter (Chen, 1997; Khani et al., 2012;
359 Kunioka et al., 2006)

360 **4.2. Environmental control on coral Na/Ca ratios**

361 **4.2.1. Salinity**

362 Recently, Na/Ca ratios in foraminiferal calcite have been suggested as a potential salinity proxy
363 (Allen et al., 2016; Bertlich et al., 2018; Mezger et al., 2016; Wit et al., 2013). Ishikawa and
364 Ichikuni (1984) proposed that the activity of Na in seawater is the primary controlling factor for
365 the incorporation of Na in calcite. However, more recent studies have shown that Na/Ca in
366 foraminiferal calcite is mainly driven by the seawater Na/Ca ratio instead of the Na activity

367 when this is the dominant variable (Evans et al., 2018; Hauzer et al., 2018). Species-specific
368 offsets make further biological controls highly plausible.

369 In this study, no correlation between salinity and Na/Ca ratios is present (Fig. 3). The positive
370 trend up to 35 g/kg followed by a negative trend after 35 g/kg can be explained by growth rate
371 changes due to the changing salinity. To our knowledge no studies on the effect of salinity on
372 growth rates have been conducted on *D. pertusum* but it is plausible that it shows reduced
373 growth rates in salinities diverging from the biological optimum similar to other marine
374 organisms (e.g. *M. edulis* (Malone and Dodd, 1967)). A specific osmoregulation is probably
375 not needed for CWC in the mostly salinity stable habitats they live in (Roberts et al., 2009).
376 Reduced growth rates consequently lower the amount of lattice defects and the amount of
377 possible incorporation sites for sodium (Mucci, 1988; White, 1977; Yoshimura et al., 2017), if
378 bulk extension-rates are indeed related to crystal growth rates.

379 If Na/Ca ratios in corals are controlled by calcification rates, a calcification rate proxy could be
380 used to correct this effect. Sr/Ca ratios have been discussed as a possible growth rate proxy
381 (de Villiers et al., 1994) and may be used to determine changes in growth rate. However, our
382 data shows that the Sr/Ca ratios remain constant with changing salinities. Accordingly,
383 concluding from the results of de Villiers et al. (1994) the calcification rate would remain
384 constant over the whole salinity range. It should be noted that higher growth rates do not
385 necessarily imply higher calcification rates or vice versa. Higher growth rate can also be
386 caused by higher organic deposits in the skeleton (Stolarski, 2003). Therefore, a change in
387 calcification cannot necessary be inferred from changing Sr/Ca ratios. Still, the effects that
388 growth or calcification rate changes and the different skeletal architectures have on Sr/Ca
389 ratios in corals is still discussed. There is evidence for positive and negative correlation of
390 Sr/Ca with growth and calcification rate as well as the different skeletal architectures (Allison
391 and Finch, 2004; Cohen et al., 2006; Kunioka et al., 2006; Raddatz et al., 2013). It still remains
392 unknown why there is no persistent Sr/Ca variation between the differential skeletal
393 architectures (COC, fibrous deposits) in this study despite being visible in several other studies

394 (Cohen et al., 2006; Gagnon et al., 2007; Raddatz et al., 2013). An explanation could be the
395 low sampling resolution in the profiled samples and possible mixing of COC and fibrous zone
396 material. Further research is needed to evaluate the effects of growth and calcification rates
397 on Sr/Ca ratios in biogenic carbonates.

398 **4.2.2. Temperature**

399 A temperature control on Na/Ca ratios has been shown in inorganic precipitated aragonite
400 (White, 1977) and in the planktonic foraminifera *G. ruber* and *G. sacculifer* (Mezger et al.,
401 2016), although temperature and salinity covary in that study. Furthermore, Rollion-Bard and
402 Blamart (2015) suggest a possible temperature control on Na/Ca ratios in the CWC *D.*
403 *pertusum* and the warm-water coral *Porites* sp. However, the temperature sensitivity in
404 inorganically precipitated aragonite is far lower compared to the biogenic aragonite from CWC
405 including a systematic offset of $K_d^{Na}_{(15^\circ C)} = 1.17 \cdot 10^{-4}$. Interestingly, other marine carbonates
406 (*Porites* sp., *M. edulis*) also fit in the calculated temperature sensitivity. This holds true for
407 biogenic aragonite and biogenic calcite, where *M. edulis* fits into the temperature sensitivity
408 found by Mezger et al. (2016). A combined regression using the data from Evans et al. (2018),
409 Mezger et al. (2016) and Lorens and Bender (1980) reveals a temperature sensitivity of -0.37
410 mmol/mol/°C which is strikingly similar to the sensitivity in aragonite of -0.31 mmol/mol/°C (Fig.
411 6). The samples that Mezger et al. (2016) used in their study derive from the Red Sea, where
412 a negative correlation between the seawater salinity and seawater temperature exists. They
413 conclude that the salinity effect on Na/Ca ratios and the covariance between salinity and
414 temperature cause the temperature sensitivity of Na/Ca ratios. However, it is also possible that
415 the salinity sensitivity is caused by a temperature effect.

416 The apparent offset between inorganically precipitated aragonite and biogenic carbonates
417 further implies a biological control on Na incorporation. In contrast to other elements such as
418 Lithium (Montagna et al., 2014), the high correlation between *D. pertusum*, *M. oculata*,
419 Caryophylliidae, *Porites* sp. and *M. edulis* implies that the Na/Ca variance introduced by these
420 possibly occurring vital effects appear to be similar for all these species. We suggest that

421 similar Na pathways into the calcifying space exist in foraminifera, mussels and scleractinian
422 warm-water as well as cold-water corals and temperature exerts a strong control on the activity
423 of these pathways, altering the sodium availability during calcification. Further controls are
424 possibly contributed by temperature dependent solubility variations of CaCO_3 and Na_2CO_3 and
425 an exothermic Na incorporation mechanism.

426 Bertlich et al. (2018) proposed that lower temperatures increase the solubility of calcium
427 carbonate and increase the amount of free Ca, leading to higher Na/Ca ratios at lower
428 temperatures. Yet such a solubility-controlled temperature effect on calcite and aragonite is
429 rather small, whereas the sensitivity to pressure changes is much more pronounced
430 (Pytkowicz and Conners, 1964; Zeebe and Wolf-Gladrow, 2001). Accordingly, the Na/Ca ratio
431 should also decrease with water depth. Here we do observe a relationship between Na/Ca
432 ratios and water depth, but at constant temperatures ($7.2^\circ\text{C} - 7.8^\circ\text{C}$) there is no effect of water
433 depth (160 m – 280 m) on Na/Ca ratios. The relationship between depth and Na/Ca ratios is
434 therefore presumably caused by the positive correlation between water temperature and water
435 depth. A decrease in Na/Ca ratios with temperatures could also be explained by solubility
436 effects similar to the effects that are discussed to cause the temperature effects on Li/Ca ratios
437 (Marriott et al., 2004). The solubility of Na_2CO_3 increases with increasing temperature (Haynes
438 et al., 2016). Again, this would result in decreasing Na/Ca ratios with increasing temperature,
439 because the solubility of Na_2CO_3 decreases relative to calcium carbonate (Haynes et al.,
440 2016), making it thermodynamically less favorable to incorporate Na. The effects of pressure
441 on the solubility of Na_2CO_3 cannot be quantified at the moment due to the lack of studies.

442 Moreover, the temperature effect can also be caused by an exothermic substitution
443 mechanism of Na into the aragonite lattice, similar to the incorporation of Mg in calcite (Mucci
444 and Morse, 1990). If the substitution between Ca and Na is exothermic, consequently the
445 incorporation of Na is favored at lower temperatures. However, there is to our knowledge, no
446 study available that contains enthalpy data for this reaction. While the proposed mechanism
447 by Bertlich et al., (2018) can be excluded as an explanation for the temperature sensitivity of

448 Na/Ca ratios, the other explanations are equally plausible in terms of the existing studies. Still,
449 the differences in the temperature sensitivity between inorganic precipitated aragonite and
450 biogenic aragonite requires further biological controls to explain this deviation.

451 As an alternative, we explore whether temperature dependent Na membrane pathways can
452 explain temperature effects on aragonitic Na/Ca ratios. There are several enzymes and ion
453 pumps known that constitute sodium pathways through the membrane of the calcifying space.
454 Na^+/K^+ -ATPase are known from the tropical coral *Galaxea fascicularis* (Ip and Lim, 1991),
455 Na/Ca ion pumps are suggested to exist in *Galaxea fascicularis* and *Tubastraea faulkneri*
456 (Marshall, 1996). Na^+/K^+ -ATPase was found in the bivalve species *M. edulis* and *Limecola*
457 *balthica* (Pagliarani et al., 2006; Wang and Fisher, 1999) as well as Na/Mg ion pumps in
458 *Ruditapes philippinarum* and *Mytilus galloprovincialis* (Pagliarani et al., 2006). Whether these
459 enzymes exist in *D. pertusum* is unknown, but since corals possess a nervous system (Chen
460 et al., 2008) and *D. pertusum* shows reaction to electrical stimulation (Shelton, 1980) at least
461 the existence of Na^+/K^+ -ATPase must be assumed. However, it remains unclear if this enzyme
462 participates in the modification of the calcifying fluid. The participation of Na/Ca ion pumps is
463 also plausible, since it would result in higher Ca-concentrations in the calcifying space which
464 would aid the calcification process due to the high transport capacity (Carafoli et al., 2001).
465 Membrane calcium pumps on the other hand are better suited to transport Ca from a
466 compartment with low Ca-concentrations, which is not applicable when considering seawater
467 as the source compartment (Wang et al., 1992). Since the activity of enzymes is a function of
468 temperature (Sizer, 2006), a temperature control of the ion concentration in the calcifying fluid
469 has to be considered. Rising temperatures would increase the activity of the particular enzyme
470 following the Arrhenius equation (Arrhenius, 1896) and consequently lower the Na-
471 concentration in the calcifying space. Unfortunately, it is impossible to quantify these effects
472 from the data at hand, because the optimum temperature and activation energy is not enzyme
473 specific, but further controlled by enzyme and substrate purity and the presence of inhibitors
474 or activators. Specific research is needed to identify the particular enzyme in these corals as
475 well as determine the rate of ion-exchange, although we note that an enzymatic control on

476 aragonitic Na/Ca ratios does not necessarily imply a temperature control. In addition, besides
477 a temperature control, there is also a pH control on enzyme activity (Trivedi and Danforth,
478 1966). While a positive correlation between Na/Ca and seawater pH is present in the samples
479 utilized here, it is not possible to determine if this is caused by pH-controlled enzymatic activity
480 or due to an increased calcification rate. Higher seawater pH would cause higher calcification
481 fluid pH which would consequently also increase the aragonite saturation in the calcifying fluid
482 (McCulloch et al., 2012). The degree of pH elevation in the coral calcifying space would
483 therefore decrease, ultimately conserving energy ($\approx 10\%$ / $-0.1 \text{ pH}_{\text{SW}}$) which can be used for
484 ATP-dependent transport proteins, pumping more Ca or CO_3^{2-} , leading to faster calcification
485 (McCulloch et al., 2012). It is also possible that the apparent sensitivity of Na/Ca to pH changes
486 is caused by the negative covariance of pH and temperature

487 Admittedly, the above discussion is only viable under the assumption of a closed calcifying
488 space with a much lower $[\text{Na}]_{\text{ECF}}$ than $[\text{Na}]_{\text{Seawater}}$. In the case of an open or semi-enclosed
489 calcifying space with $[\text{Na}]_{\text{ECF}}$ close or equal to $[\text{Na}]_{\text{Seawater}}$ the amount of Na removed by
490 enzymes or other ion-pumps is far too low to cause any significant changes in the composition
491 of the calcifying fluid with regards to Na. In combination with the low distribution coefficient,
492 changes in the Na-concentration of the ECF cannot cause the high variability of the skeletal
493 Na/Ca ratios. Since there is evidence for an at least semi-enclosed calcifying space (Tambutté
494 et al., 2011) we also consider this option. As described in Sec. 3.3 it is possible to calculate
495 the Mg-concentration of the ECF under the assumption of seawater leakage into the calcifying
496 space (Adkins et al., 2003; Gagnon et al., 2012) and a resulting approximately constant Na-
497 concentration. Based on this hypothesis, and the calculations defined in Eq. 3 and 4, we show
498 that the Mg-concentration in the ECF is constant, but with changing Ca-concentration (Fig. 7).
499 There is a large degree of scatter in the $[\text{Mg}]_{\text{ECF}}$ reconstructions (Fig. 7), which we suggest is
500 unlikely to represent real changes in the ECF $[\text{Mg}]$ as it is difficult to envisage a purpose for
501 elevating $[\text{Mg}]_{\text{ECF}}$ above the of seawater given that it plays an inhibitory role in calcium
502 carbonate precipitation **by acting antagonistic to the calcium transport (Okazaki, 1956; Swart,**
503 **1981; Yamazato, 1966)**. It may be that the scatter above seawater values is derived from the

504 presence of organic material, as a small positive bias in measured coral Mg/Ca would result in
505 a large overestimation of $[Mg]_{ECF}$. Crucially however, we find that $[Mg]_{ECF}$ does not change as
506 a function of $[Ca]_{ECF}$, with the implication that in this model changing skeletal Mg/Ca and Na/Ca
507 ratios are not caused by changes of the Mg or Na-concentration of the ECF but rather are
508 entirely explicable through changes in the Ca-concentration. Again, this might be caused by
509 temperature-dependent enzyme or ion-pump activity. Higher temperatures would then cause
510 a higher exchange capacity (Elias et al., 2001), leading to higher Ca- (Fig. 7) and marginally
511 lower Na-concentrations in the ECF and consequently lower Mg/Ca and Na/Ca ratios. An
512 elevation of $[Ca]$ in the ECF and the calcifying front is also supported by recent studies from
513 Decarlo et al., (2018) and Sevilgen et al., (2019), who conducted Raman spectroscopic, $\delta^{11}B$
514 and microsensor measurements on *Pocillopora damicornis*, *Acropora youngei* and *Stylophora*
515 *pistilla*. The results furthermore indicate the involvement of transcellular pathways to elevate
516 the Ca-concentration in the ECF (Sevilgen et al., 2019).

517 Even though a clear correlation between temperature and Na/Ca is present, the usefulness of
518 Na/Ca ratios is greatly reduced due to the large intraspecies variability. At 6°C Na/Ca ratios
519 vary by up to 20% and even up to 10 % in a single polyp. There are several possible reasons
520 for this variability. One is the insufficient removal of the COC during the sampling process. Due
521 to the high growth rate and high organic content in the COC, elements, such as Mg, Na and Li
522 are enriched whereas other like U are depleted (Gagnon et al., 2007; Raddatz et al., 2013,
523 2014b; Robinson et al., 2014; Rollion-Bard and Blamart, 2014, 2015). This effect would also
524 explain the high Na/Ca values in corals from the Mediterranean Sea ($T=13.56^{\circ}C$). It is possible
525 that during the sampling process a larger amount of the fibrous deposits was removed in
526 comparison to the other samples. This would cause a greater effect of the enriched COC
527 material and therefore cause higher Na/Ca ratios. It is therefore preferable to use in-situ
528 techniques (laser ablation, EPMA, SIMS) instead of solution-based chemistry and profile
529 measurements through the theca wall instead of bulk samples, because it allows for a better
530 recognition and removal of values that derive from COC or COC-like structures. Seasonality
531 could be also a factor responsible for a percentage of the variation, but the sampled corals

532 originate from depths where seasonality presumably only plays a minor role. An estimated
533 seasonal temperature change of 4°C only suffices to explain 1 mmol/mol variation but not the
534 observed variation of 10 mmol/mol. From this, it can be inferred that there must be other
535 controls on Na/Ca ratios besides water temperature. Diurnal temperature fluctuations caused
536 by internal waves as found for example in the Rockall Trough are also not high enough (3°C)
537 to explain these variations (Mienis et al., 2007). As mentioned in Sec 4.1, calcification rates
538 constitute a major control on Na/Ca ratios by controlling the amount of incorporation sites for
539 Na (Kitano et al., 1975; Mucci, 1988; White, 1977; Yoshimura et al., 2017). Therefore,
540 numerous second order control factors could cause variations in the Na/Ca ratios by controlling
541 the calcification rate. These second order controls include nutrient availability and supply,
542 changes in the carbonate system, coral fitness and many more. Some of these controls
543 (nutrient supply, coral fitness) have the potential to vary with a high spatial resolution and
544 consequently cause great variations in Na/Ca ratios even if the samples derive from the same
545 colony.

546 **4.3. Na/Mg ratios to overcome vital effects**

547 Even though a good correlation of $R^2=0.9$ between Na/Ca and temperature is observable in
548 our data, the samples from the Mediterranean Sea ($T=13.54^\circ\text{C}$) show slightly elevated Na/Ca
549 ratios. Reasons for this are discussed in Sec. 4.2. Rollion-Bard and Blamart (2015) proposed
550 Na/Mg ratios to overcome these effects. The basis for this is that Na/Ca and Mg/Ca ratios
551 could be controlled by similar vital effects such as growth rate and the amount of organic
552 content. **Combining Na/Ca and Mg/Ca ratios reduces the impact of these effects, though the**
553 **temperature sensitivity of Na/Ca ratios is preserved as Mg/Ca ratios show no apparent**
554 **correlation with temperature (Fig. 8).** The resulting regression between Na/Mg and
555 temperature yields the following equation:

$$556 \quad f_{T_{6-22^\circ\text{C}}} = 7.1 \pm 0.17 - 0.07 \pm 0.01 \times T \quad (R^2 = 0.92, P = 0.009) \quad (5)$$

557 The application of Na/Mg in this study does not significantly improve the regression, as it
558 removes the inverse correlation between 6 and 10°C. This might be caused by covariance

559 between sodium and magnesium. It was shown that magnesium in the parent solution reduces
560 the amount of incorporated sodium (Okumura and Kitano, 1986). However, utilizing Na/Mg
561 ratios removes the striking irregularity at 13.54 °C. The large scatter, however, is not
562 significantly reduced which implies further vital effects that cannot be resolved with this
563 technique. To overcome this the mean of at least 10 analyzed samples should be used to
564 obtain reliable results. If these prerequisites are fulfilled, Na/Mg and Na/Ca could provide a
565 means of reconstructing temperature. This could prove useful especially for temperature
566 reconstructions in deep time on organisms that are extinct today. In this case the nearest living
567 relative principle is used, which potentially introduces large errors. Further research on
568 different aragonitic and calcitic organisms is necessary to detect further species that show the
569 same temperature sensitivity. If it is shown that Na/Ca and/or Na/Mg ratios show no species-
570 specific variations, empirical calibrations could be applied to extinct species for which proxy
571 calibrations are not possible. Still though, when using Na/Ca for temperature reconstructions
572 changes in seawater have to be considered that would lead to an underestimation of
573 temperature at high pH. However, Na/Mg show no sensitivity to changes in seawater pH, so
574 by combining Na/Ca and Mg/Ca ratios this effect can be ignored.

575 **5. Conclusion**

576 The data at hand does not support the utility of Na/Ca in cold-water corals as a salinity proxy
577 as proposed by Wit et al., (2013) and Mezger et al., (2016) for biogenic calcite. While there is
578 a positive trend between Na/Ca and salinity when excluding data from the Red Sea samples,
579 it is not statistically significant.

580 A significant inverse correlation between temperature and Na/Ca ratios is present, which
581 cannot be explained by a co-variance of temperature and salinity (c.f. Mezger et al., 2016).
582 Two additional organisms, *Porites* sp. (Mitsuguchi et al., 2001; Ramos et al., 2004) and *M.*
583 *edulis* (Lorens and Bender, 1980) fit in this regression too. The mechanism of sodium
584 incorporation therefore appears to be consistent between these three species. We propose
585 temperature-dependent activity in Na-ion or Ca-ion transport proteins as the underlying

586 mechanism behind the observable correlation. While the intraspecies and intraindividual
587 variation is large, Na/Ca can be well correlated to environmental variables when based on the
588 averages of several specimens. Therefore, Na/Ca ratios might provide a temperature-proxy
589 that is usable for a wide variety of aragonitic organisms and maybe even calcitic organisms.
590 As proposed by Rollion-Bard and Blamart (2015), Na/Mg ratios can be used to correct for
591 inconsistencies during the sampling process.

592 **Author contribution**

593 Jacek Raddatz and Nicolai Schleinkofer designed the experiments and conducted the
594 measurements. Jacek Raddatz, Andre Freiwald, Lydia Beuck, Andres Rüggeberg and Volker
595 Liebetrau provided samples and environmental data. Nicolai Schleinkofer prepared the
596 manuscript with contributions from all co-authors.

597 **Competing interests**

598 The authors declare that they have no conflict of interest.

599 **Data availability**

600 Measured data is available through the supplementary material.

601 **Acknowledgements**

602 We are grateful to all cruise captains, crew members and cruise participants of research
603 cruises POS325, POS391, POS455, POS 385, M61, POS625, B10-17a/b, 64PE284, M70/1,
604 COR2, MSM20-4, KRSE2013 and RV Gunnerus. Ship time of RV Belgica was provided by
605 BELSPO and RBINS–OD Nature. Cruise POS391 was realized by DFG Project RI 598/4-1.
606 JR acknowledges funding from DFG project ECHO RA 2516-1. AR acknowledges support from
607 Swiss National Science Foundation, SNF project number 200021_149247.

608 FIERCE is financially supported by the Wilhelm and Else Heraeus Foundation, which is
609 gratefully acknowledged. This is FIERCE contribution No. 002

610

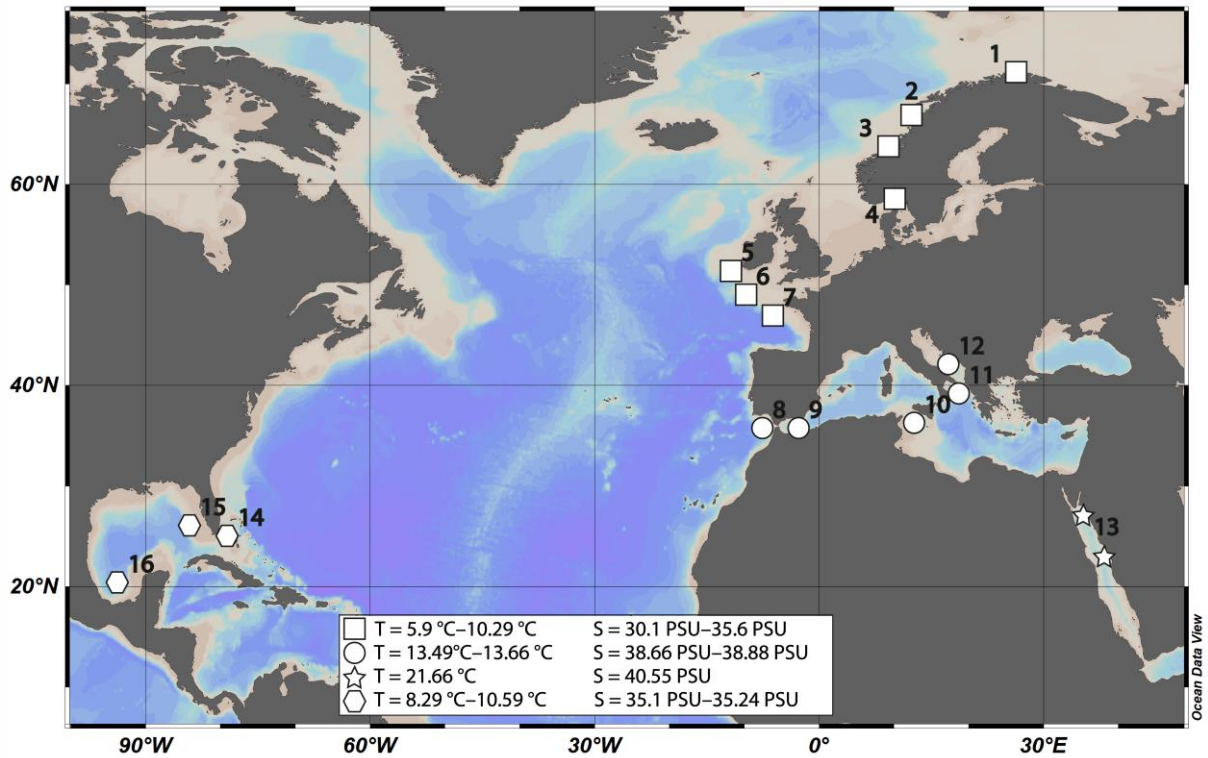
611

612

613

614

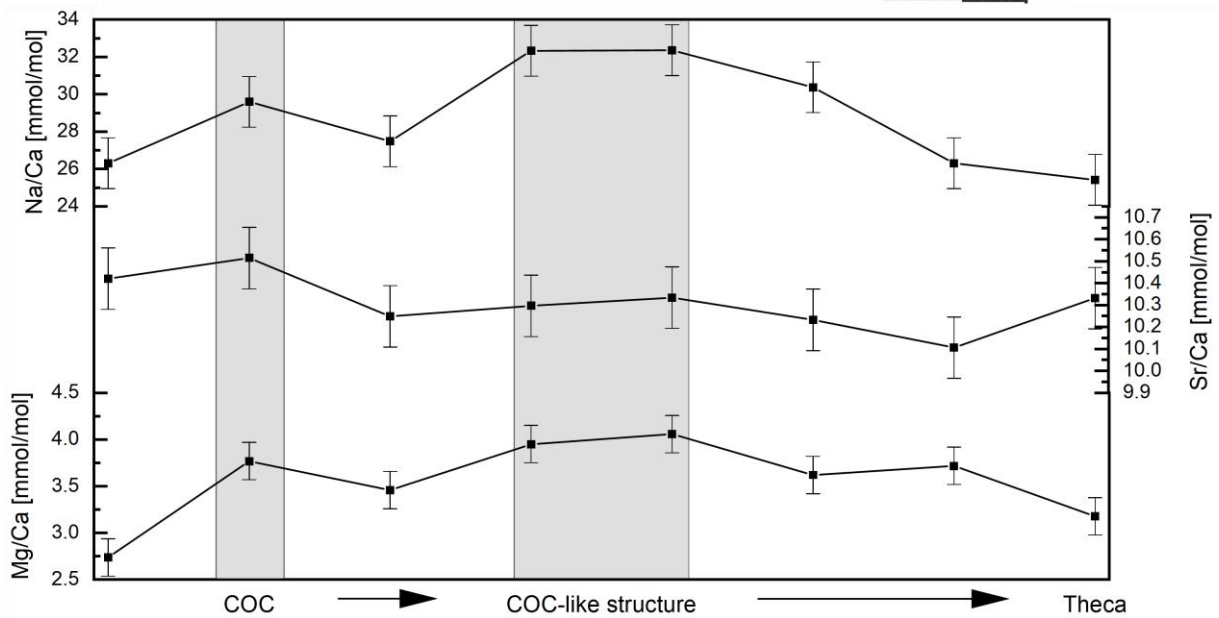
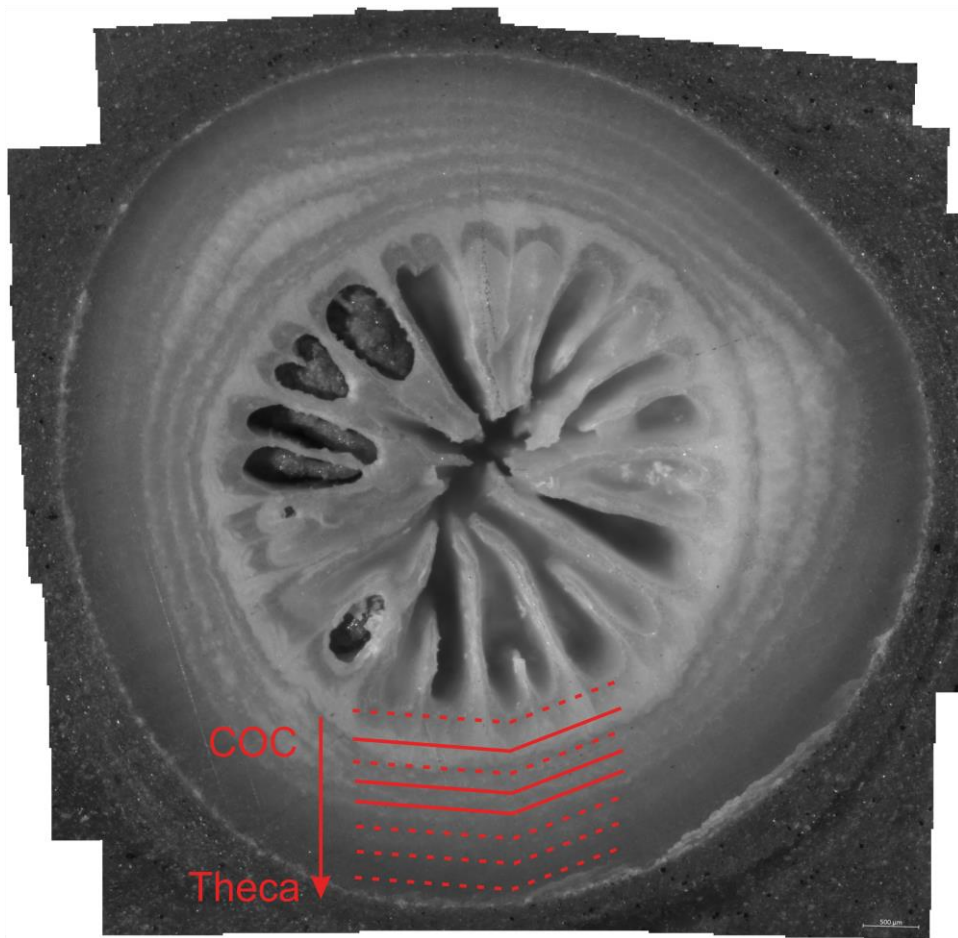
615 **Figures**



616

617 **Figure 1** Map of sampling locations. Locations are grouped in four areas with similar physical parameters.
 618 **1:** LoppHAVet, Sotbakken, Stjernesund; **2:** Traenadjupet; **3:** Sula, Nordleksa, Tautra, Røberg; **4:** Oslofjord; **5:**
 619 Galway Mound, **6:** Whittard Canyon; **7:** Guilvinec Canyon; **8:** Meknes Carbonate Mound Province **9:** El Idrissi
 620 Bank; **10:** Urania Bank; **11:** Santa Maria di Leuca (SML) Province, **12:** Bari Canyon; **13:** Red Sea; **14:** Great
 621 Bahama Bank; **15:** Southwest Florida; **16:** Campeche Bank

622



623

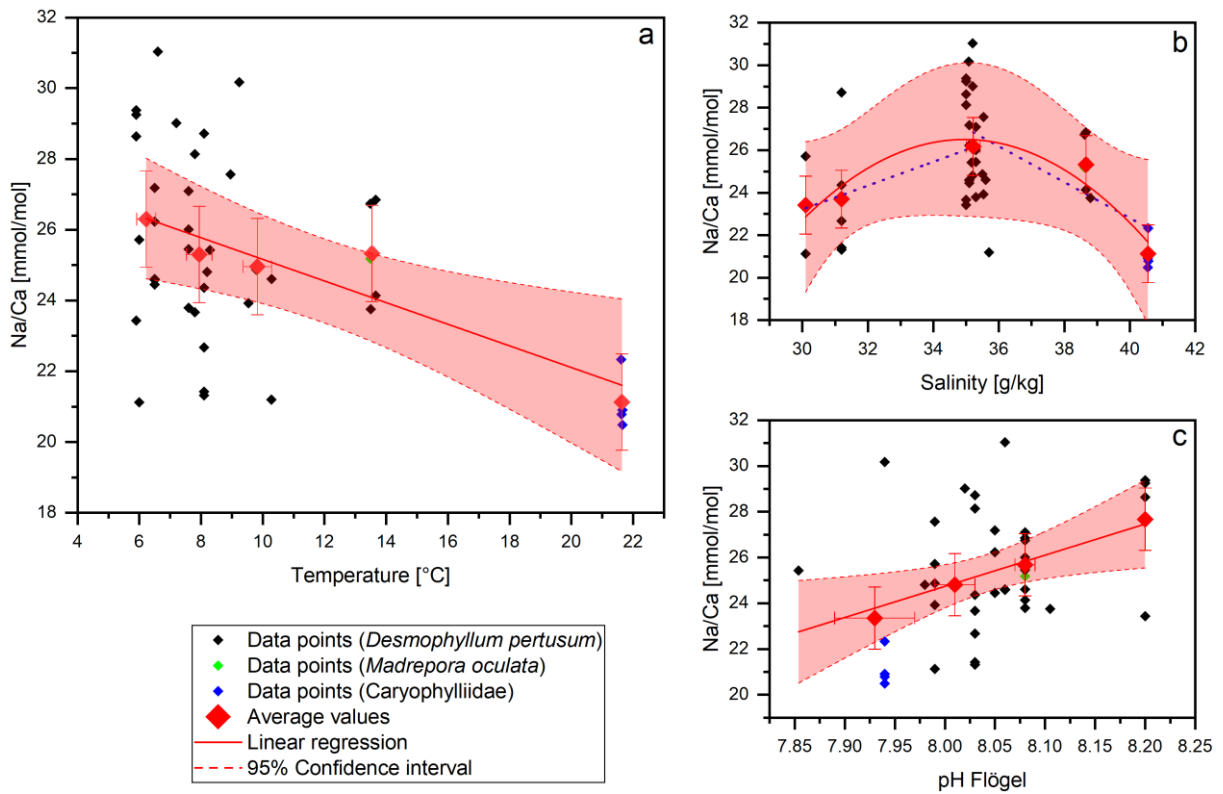
624

625

626

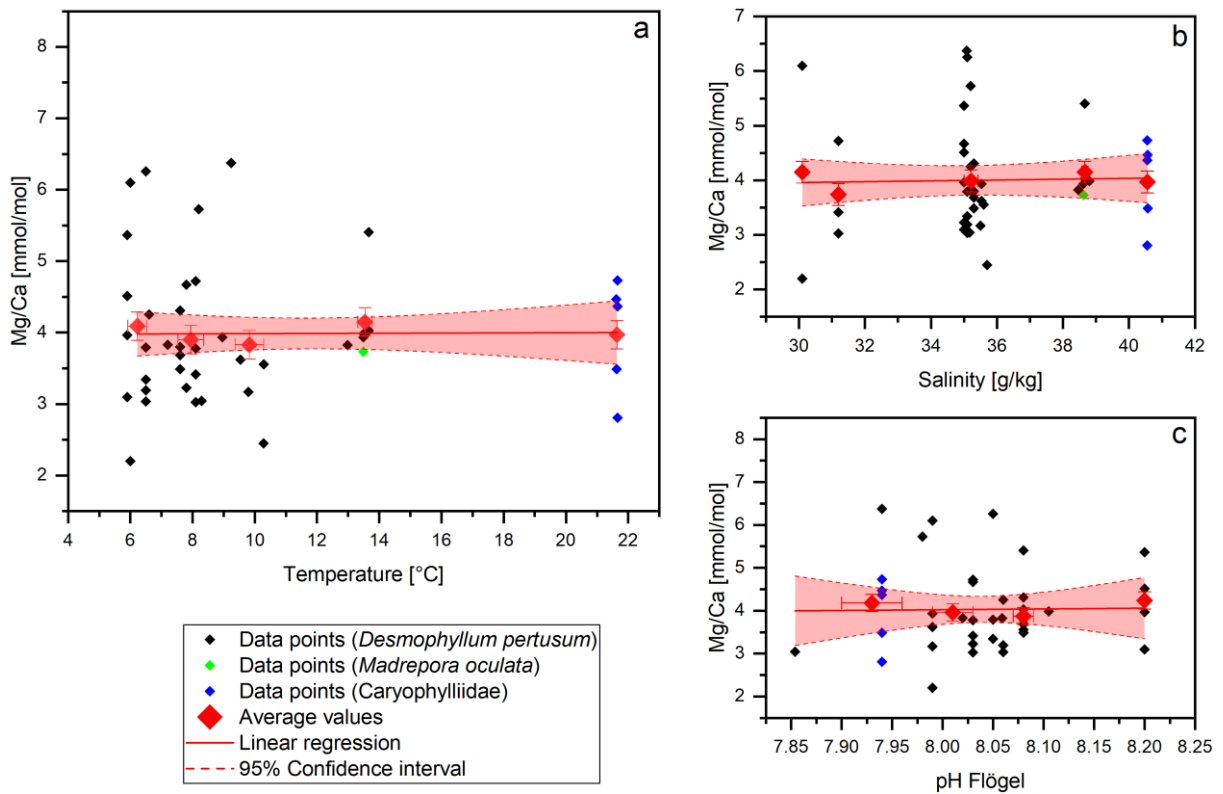
627

Figure 2 Intra-individual element heterogeneities of one sample from Lophavet (*D. pertusum*). Shaded-grey areas indicate COC and COC-like structures (solid lines in sample picture). Error bars indicate 2SD of the JCp-1 mean. Within the uncertainty Sr/Ca ratios show no significant changes throughout the coral, whereas Mg/Ca and Na/Ca show variations of 1.25 mmol/mol and 6 mmol/mol respectively.



628

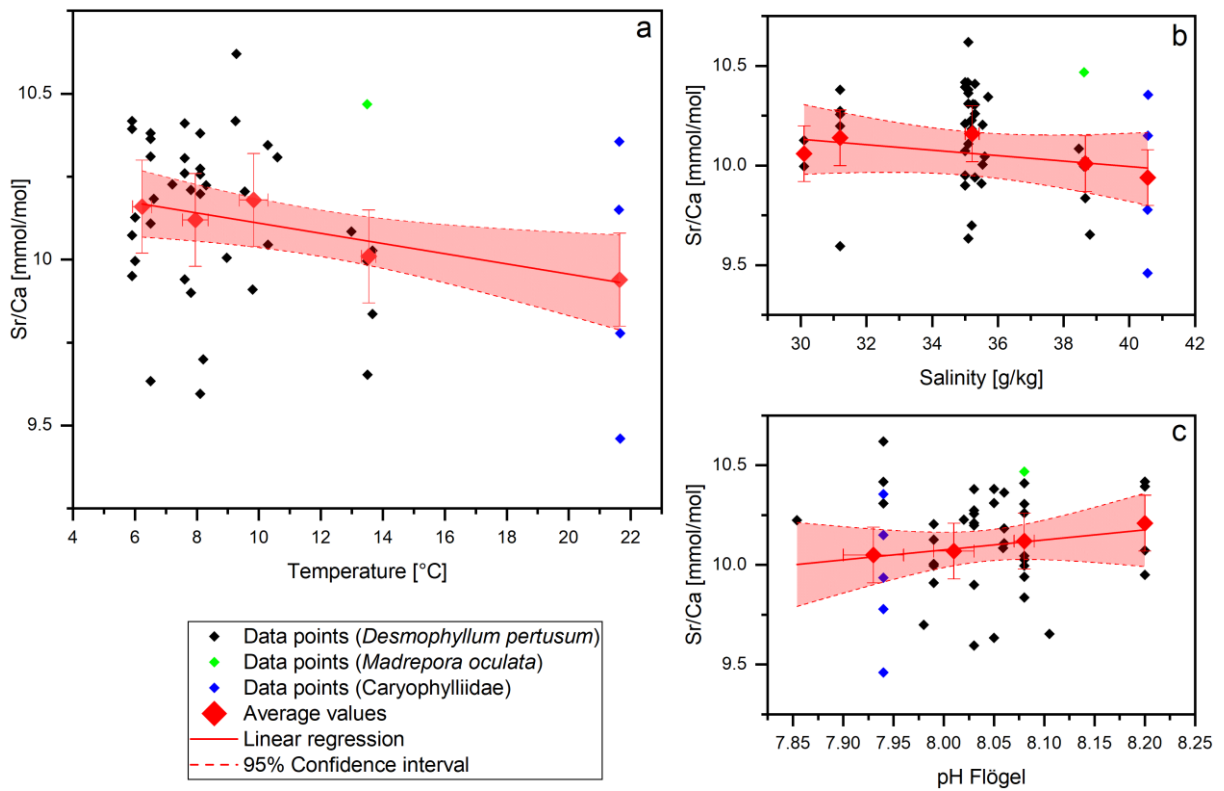
629 **Figure 3 Na/Ca Data (without COC) plotted against water temperature, salinity and pH. Red diamonds**
 630 **indicate averaged values for temperature ranges. Temperature ranges are 5–7°C, 7–9°C, 9–11°C, 13–15°C**
 631 **and 21–23°C. X-Error relates to the SD of the temperature/salinity mean. Y- Error bars indicate 2SD of the**
 632 **JCp-1 mean. Red lines are linear regressions of the averaged values with the 95 % confidence interval**
 633 **shaded. Blue dotted lines indicate linear regressions for different salinity ranges.**



634

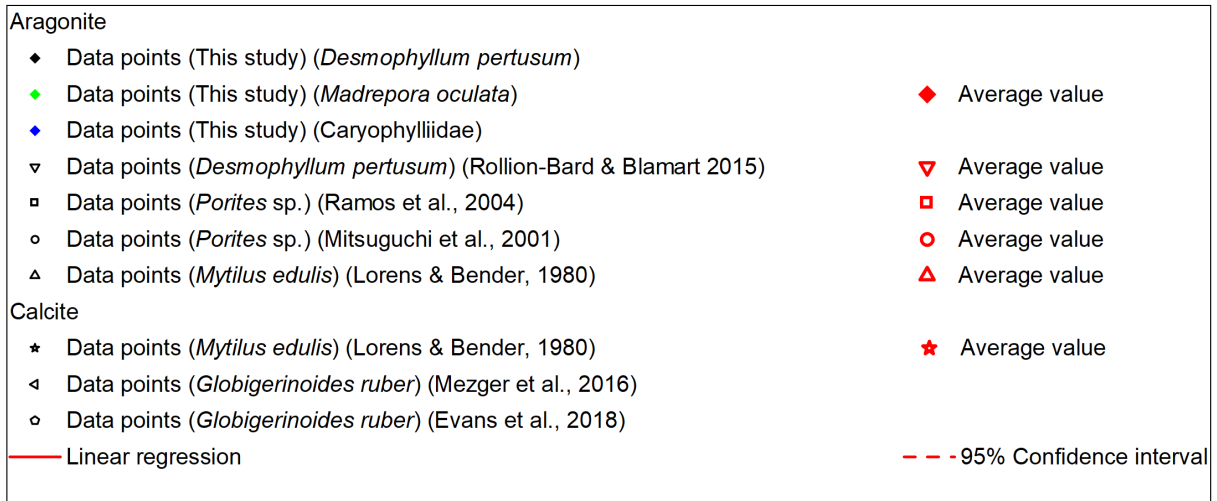
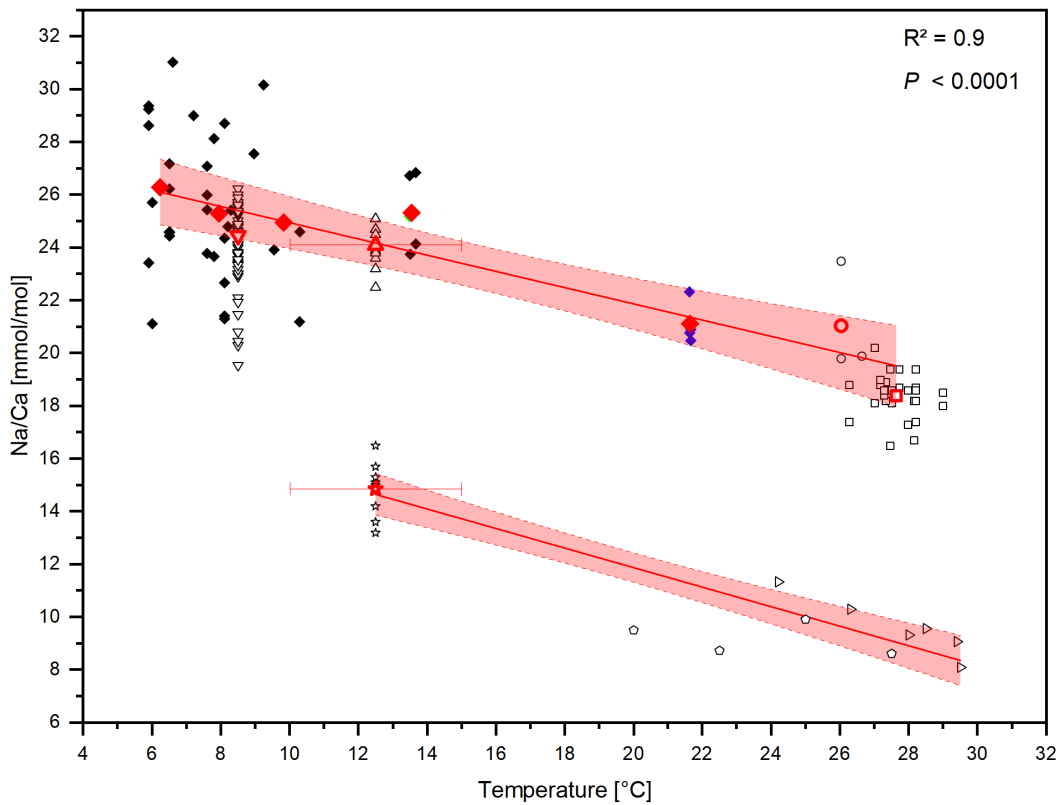
635 **Figure 4 Mg/Ca Data (without COC) plotted against water temperature, salinity and pH. Red diamonds**
 636 **indicate averaged values for temperature ranges. Temperature ranges are 5–7°C, 7–9°C, 9–11°C, 13–15°C**
 637 **and 21–23°C. X-Error relates to the SD of the temperature/salinity mean Y- Error bars indicate 2SD of the**

638 JCp-1 mean. Red lines are linear regressions of the averaged values with the 95 % confidence interval
 639 shaded.



640

641 Figure 5 Sr/Ca Data (without COC) plotted against water temperature, salinity and pH. Red diamonds
 642 indicate averaged values for temperature ranges. Temperature ranges are 5–7°C, 7–9°C, 9–11°C, 13–15°C
 643 and 21–23°C. X-Error relates to the SD of the temperature/salinity mean. Y- Error bars indicate 2SD of the
 644 JCp-1 mean. Red lines are linear regressions of the averaged values with the 95 % confidence interval
 645 shaded.



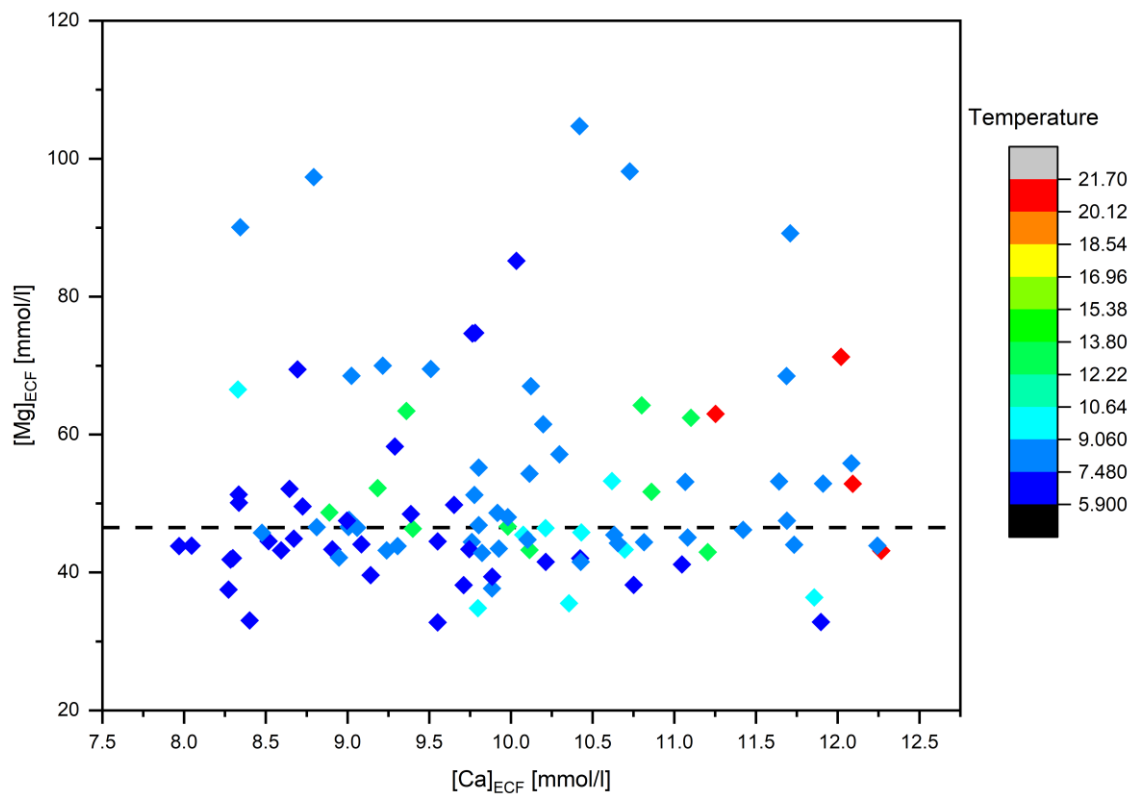
646

647 Figure 6 Compiled Na/Ca ratios from different studies. *D. pertusum*, *M. oculata*, *M. edulis* and *Porites* sp.
 648 show a negative linear relation with water temperature. R^2 relates only to the aragonitic samples
 649 Calcitic samples from *M. edulis* and *Globigerinoides ruber* show the same sensitivity, albeit with an offset of 10
 650 mmol/mol. Temperature for the data from Lorens & Bender amounts to the average temperature of the tank
 651 the corals were cultivated in while the error bars show maximum and minimum values.

652

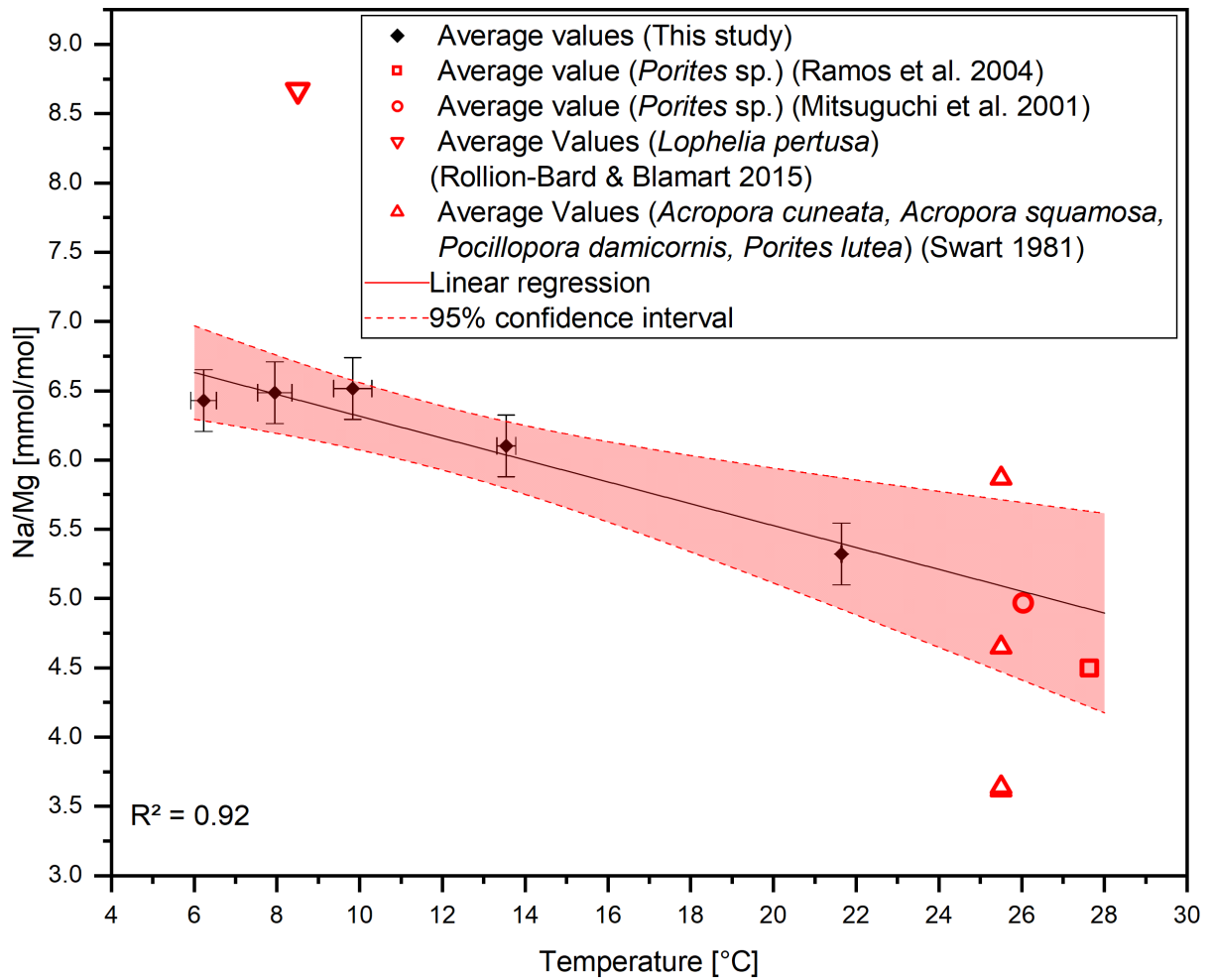
653

654



655

656 **Figure 7 Calcium and Magnesium concentration in the ECF of the investigated corals. The color of the**
 657 **data points indicate the ambient water temperature, which is increasing with increasing Ca-**
 658 **concentrations. The dashed line indicates the median of the Mg-concentration in the ECF.**



659

660 **Figure 8 Na/Mg ratios from this study vs. water temperature. Na/Mg ratios can be used to correct for the**
 661 **sampling of varying proportions of different domains. Y-Error bars relate to 2SD of the JCp-1**
 662 **measurements. X-Error bars relate to 1SD of the temperature mean for the chosen temperature ranges.**

663

664

665

666

667

668

669

670

671

672

673

674

675

676

677 **Tables**

Temperature [°C]	Na/Ca			Sr/Ca			Mg/Ca		
	mmol/mol	n	SD	mmol/mol	n	SD	mmol/mol	n	SD
6.23 ± 0.31	26.30	12	2.88	10.16	12	0.23	4.09	12	1.27
7.94 ± 0.41	25.30	15	2.48	10.13	15	0.24	3.90	14	0.74
9.83 ± 0.46	24.96	5	3.26	10.18	5	0.21	3.83	5	1.49
13.56 ± 0.09	25.33	5	1.43	10.01	6	0.27	4.15	6	0.62
21.64 ± 0.02	21.13	4	0.82	9.94	5	0.34	3.97	5	0.8
Average Salinity [g/kg]	Na/Ca			Sr/Ca			Mg/Ca		
	mmol/mol	n	SD	mmol/mol	n	SD	mmol/mol	n	SD
30.1	23.42	2	2.25	10.06	2	0.09	4.15	2	2.75
31.2	23.70	5	3.06	10.14	5	0.31	3.74	4	0.73
35.22 ± 0.21	26.18	25	2.46	10.16	25	0.22	3.99	25	1.01
38.67 ± 0.07	25.33	5	1.43	10.01	6	0.27	4.16	6	0.62
40.56 ± 0.01	21.13	4	0.82	9.94	5	0.34	3.97	5	0.8

678 **Table 1 Na/Ca, Sr/Ca, Mg/Ca mean values measured with ICP-OES, standard deviation and sample number.**
679 **Values relate to certain salinity and temperature envelopes.**

680

681

682

683

684

685

686

687

688

689

690

691

692

693

694 **References**

- 695 Adkins, J. F., Boyle, E. A., Curry, W. B. and Lutringer, A.: Stable isotopes in deep-sea corals
 696 and a new mechanism for “vital effects,” *Geochim. Cosmochim. Acta*, 67(6), 1129–1143,
 697 doi:10.1016/S0016-7037(00)01203-6, 2003.
- 698 Al-Horani, F. A., Al-Moghrabi, S. M. and De Beer, D.: The mechanism of calcification and its
 699 relation to photosynthesis and respiration in the scleractinian coral *Galaxea fascicularis*, *Mar.*
 700 *Biol.*, 142(3), 419–426, doi:10.1007/s00227-002-0981-8, 2003.
- 701 Allemand, D., Tambutté, É., Zoccola, D. and Tambutté, S.: Coral Calcification, Cells to
 702 Reefs, in *Coral Reefs: An Ecosystem in Transition*, pp. 119–150, Springer Netherlands,
 703 Dordrecht., 2011.
- 704 Allen, K. A., Hönisch, B., Eggins, S. M., Haynes, L. L., Rosenthal, Y. and Yu, J.: Trace
 705 element proxies for surface ocean conditions: A synthesis of culture calibrations with planktic
 706 foraminifera, *Geochim. Cosmochim. Acta*, 193, 197–221, doi:10.1016/j.gca.2016.08.015,
 707 2016.
- 708 Allison, N. and Finch, A. A.: High-resolution Sr/Ca records in modern *Porites lobata* corals:
 709 Effects of skeletal extension rate and architecture, *Geochemistry, Geophys. Geosystems*,
 710 5(5), doi:10.1029/2004GC000696, 2004.
- 711 Amiel, A. J., Friedman, G. M. and Miller, D. S.: Distribution and nature of incorporation of
 712 trace elements in modern aragonitic corals*, *Sedimentology*, 20(1), 47–64,
 713 doi:10.1111/j.1365-3091.1973.tb01606.x, 1973.
- 714 Anagnostou, E., Sherrell, R. M., Gagnon, A., LaVigne, M., Field, M. P. and McDonough, W.
 715 F.: Seawater nutrient and carbonate ion concentrations recorded as P/Ca, Ba/Ca, and U/Ca
 716 in the deep-sea coral *Desmophyllum dianthus*, *Geochim. Cosmochim. Acta*, 75(9), 2529–
 717 2543, doi:10.1016/j.gca.2011.02.019, 2011.
- 718 Anagnostou, E., Huang, K. F., You, C. F., Sikes, E. L. and Sherrell, R. M.: Evaluation of
 719 boron isotope ratio as a pH proxy in the deep sea coral *Desmophyllum dianthus*: Evidence of
 720 physiological pH adjustment, *Earth Planet. Sci. Lett.*, 349–350(July 2015), 251–260,
 721 doi:10.1016/j.epsl.2012.07.006, 2012.
- 722 Arrhenius, S.: XXXI. On the influence of carbonic acid in the air upon the temperature of the
 723 ground, London, Edinburgh, Dublin *Philos. Mag. J. Sci.*, 41(251), 237–276,
 724 doi:10.1080/14786449608620846, 1896.
- 725 Bertlich, J., Nürnberg, D., Hathorne, E. C., De Nooijer, L. J., Mezger, E. M., Kienast, M.,
 726 Nordhausen, S., Reichart, G. J., Schönfeld, J. and Bijma, J.: Salinity control on Na
 727 incorporation into calcite tests of the planktonic foraminifera *Trilobatus sacculifer* - Evidence
 728 from culture experiments and surface sediments, *Biogeosciences*, 15(20), 5991–6018,
 729 doi:10.5194/bg-15-5991-2018, 2018.
- 730 Bett, B. J.: UK Atlantic Margin Environmental Survey: Introduction and overview of bathyal
 731 benthic ecology, *Cont. Shelf Res.*, 21(8–10), 917–956, doi:10.1016/S0278-4343(00)00119-9,
 732 2001.
- 733 Blamart, D., Rollion-Bard, C., Meibom, A., Cuif, J. P., Juillet-Leclerc, A. and Dauphin, Y.:
 734 Correlation of boron isotopic composition with ultrastructure in the deep-sea coral *Lophelia*
 735 *pertusa*: Implications for biomineralization and paleo-pH, *Geochemistry, Geophys.*
 736 *Geosystems*, 8(12), 1–11, doi:10.1029/2007GC001686, 2007.
- 737 Bollmann, J., Herrle, J. O., Cortés, M. Y. and Fielding, S. R.: The effect of sea water salinity
 738 on the morphology of *Emiliana huxleyi* in plankton and sediment samples, *Earth Planet. Sci.*
 739 *Lett.*, 284(3–4), 320–328, doi:10.1016/j.epsl.2009.05.003, 2009.

740 Brahmi, C., Kopp, C., Domart-Coulon, I., Stolarski, J. and Meibom, A.: Skeletal growth
741 dynamics linked to trace-element composition in the scleractinian coral *Pocillopora*
742 *damicornis*, *Geochim. Cosmochim. Acta*, 99, 146–158, doi:10.1016/j.gca.2012.09.031, 2012.

743 Branson, O., Bonnin, E. A., Perea, D. E., Spero, H. J., Zhu, Z., Winters, M., Hönisch, B.,
744 Russell, A. D., Fehrenbacher, J. S. and Gagnon, A. C.: Nanometer-Scale Chemistry of a
745 Calcite Biomineralization Template: Implications for Skeletal Composition and Nucleation,
746 *Proc. Natl. Acad. Sci.*, 113(46), 12934–12939, doi:10.1073/pnas.1522864113, 2016.

747 Büscher, J. V., Form, A. U. and Riebesell, U.: Interactive Effects of Ocean Acidification and
748 Warming on Growth, Fitness and Survival of the Cold-Water Coral *Lophelia pertusa* under
749 Different Food Availabilities, *Front. Mar. Sci.*, 4(April), 1–14, doi:10.3389/fmars.2017.00101,
750 2017.

751 Busenberg, E. and Niel Plummer, L.: Kinetic and thermodynamic factors controlling the
752 distribution of SO_3^{2-} and Na^+ in calcites and selected aragonites, *Geochim. Cosmochim.*
753 *Acta*, 49(3), 713–725, doi:10.1016/0016-7037(85)90166-8, 1985.

754 Carafoli, E., Santella, L., Branca, D. and Brini, M.: Generation, control, and processing of
755 cellular calcium signals, *Crit. Rev. Biochem. Mol. Biol.*, 36(2), 107–260,
756 doi:10.1080/20014091074183, 2001.

757 Chen, E., Stiefel, K. M., Sejnowski, T. J. and Bullock, T. H.: Model of traveling waves in a
758 coral nerve network, *J. Comp. Physiol. A Neuroethol. Sensory, Neural, Behav. Physiol.*,
759 194(2), 195–200, doi:10.1007/s00359-007-0305-z, 2008.

760 Chen, J.-P.: Batch and Continuous Adsorption of Strontium by Plant Root Tissues,
761 *Bioresour. Technol.*, 60, 185–189, doi:10.1016/S0960-8524(97)00021-7, 1997.

762 Cohen, A. L., Gaetani, G. A., Lundälv, T., Corliss, B. H. and George, R. Y.: Compositional
763 variability in a cold-water scleractinian, *Lophelia pertusa*: New insights into “vital effects,”
764 *Geochemistry, Geophys. Geosystems*, 7(12), doi:10.1029/2006GC001354, 2006.

765 Constantz, B. R.: Skeletal Organization in Caribbean *Acropora* Spp. (Lamarck), in *Origin,*
766 *Evolution, and Modern Aspects of Biomineralization in Plants and Animals*, pp. 175–199,
767 Springer US, Boston, MA., 1989.

768 Cuif, J.-P. and Dauphin, Y.: Microstructural and physico-chemical characterization of ‘
769 centers of calcification’ in septa of some Recent scleractinian corals, *Paläontologische*
770 *Zeitschrift*, 72(November), 257–270, doi:10.1007/BF02988357, 1998.

771 Cuif, J. P., Dauphin, Y. Y., Doucet, J., Salome, M. and Susini, J.: XANES mapping of organic
772 sulfate in three scleractinian coral skeletons, *Geochim. Cosmochim. Acta*, 67(1), 75–83,
773 doi:10.1016/S0016-7037(02)01041-4, 2003.

774 Decarlo, T. M., Comeau, S., Cornwall, C. E. and McCulloch, M. T.: Coral resistance to ocean
775 acidification linked to increased calcium at the site of calcification, *Proc. R. Soc. B Biol. Sci.*,
776 285(1878), doi:10.1098/rspb.2018.0564, 2018.

777 Druffel, E. R. M.: Geochemistry of corals: Proxies of past ocean chemistry, ocean circulation,
778 and climate, *Proc. Natl. Acad. Sci.*, 94(16), 8354–8361, doi:10.1073/pnas.94.16.8354, 1997.

779 Dullo, W. C., Flögel, S. and Rüggeberg, A.: Cold-water coral growth in relation to the
780 hydrography of the Celtic and Nordic European continental margin, *Mar. Ecol. Prog. Ser.*,
781 371, 165–176, doi:10.3354/meps07623, 2008.

782 Elderfield, H. and Ganssen, G.: Past temperature and $\delta^{18}\text{O}$ of surface ocean waters inferred
783 from foraminiferal Mg/Ca ratios, *Nature*, 405(6785), 442–445, doi:10.1038/35013033, 2000.

784 Elderfield, H., Ferretti, P., Greaves, M., Crowhurst, S. J., McCave, I. N., Hodell, D. a and
785 Piotrowski, A. M.: Evolution of ocean temperature, *Science* (80-.), 337(August), 704–709,

786 doi:10.1594/PANGAEA.786205, 2012.

787 Elias, C. L., Xue, X. H., Marshall, C. R., Omelchenko, A., Hryshko, L. V. and Tibbits, G. F.:
788 Temperature dependence of cloned mammalian and salmonid cardiac Na(+)/Ca(2+)
789 exchanger isoforms., *Am. J. Physiol. Cell Physiol.*, 281(3), C993–C1000, doi:10.1111/j.1432-
790 1033.1984.tb08031.x, 2001.

791 Von Euw, S., Zhang, Q., Manichev, V., Murali, N., Gross, J., Feldman, L. C., Gustafsson, T.,
792 Flach, C., Mendelsohn, R. and Falkowski, P. G.: Biological control of aragonite formation in
793 stony corals, *Science (80-.)*, 356(6341), 933–938, doi:10.1126/science.aam6371, 2017.

794 Evans, D., Müller, W. and Erez, J.: Assessing foraminifera biomineralisation models through
795 trace element data of cultures under variable seawater chemistry, *Geochim. Cosmochim.*
796 *Acta*, 236, 198–217, doi:10.1016/j.gca.2018.02.048, 2018.

797 Evans, D., Webb, P., Penkman, K. E. H., Kroger, R. and Allison, N.: The characteristics and
798 biological relevance of inorganic amorphous calcium carbonate (ACC) precipitated from
799 seawater, *Cryst. Growth Des.*, doi:10.1021/acs.cgd.9b00003, 2019.

800 Finch, A. A. and Allison, N.: Mg structural state in coral aragonite and implications for the
801 paleoenvironmental proxy, *Geophys. Res. Lett.*, 35(8), 1–5, doi:10.1029/2008GL033543,
802 2008.

803 Flögel, S., Dullo, W. C., Pfannkuche, O., Kiriakoulakis, K. and Rüggeberg, A.: Geochemical
804 and physical constraints for the occurrence of living cold-water corals, *Deep. Res. Part II*
805 *Top. Stud. Oceanogr.*, 99, 19–26, doi:10.1016/j.dsr2.2013.06.006, 2014.

806 Form, A. U. and Riebesell, U.: Acclimation to ocean acidification during long-term CO₂
807 exposure in the cold-water coral *Lophelia pertusa*, *Glob. Chang. Biol.*, 18(3), 843–853,
808 doi:10.1111/j.1365-2486.2011.02583.x, 2012.

809 Freiwald, A.: Reef-Forming Cold-Water Corals, in *Ocean Margin Systems*, pp. 365–385,
810 Springer Berlin Heidelberg, Berlin, Heidelberg., 2002.

811 Freiwald, A. and Roberts, J. M., Eds.: *Cold-Water Corals and Ecosystems*, Springer Berlin
812 Heidelberg, Berlin, Heidelberg., 2005.

813 Freiwald, A., Beuck, L., Rüggeberg, A., Taviani, M. and Hebbeln, D.: The White Coral
814 Community in the Central Mediterranean Sea Revealed by ROV Surveys, *Oceanography*,
815 22(1), 58–74, doi:10.5670/oceanog.2009.06, 2009.

816 Gabitov, R. I., Gaetani, G. A., Watson, E. B., Cohen, A. L. and Ehrlich, H. L.: Experimental
817 determination of growth rate effect on U⁶⁺ and Mg²⁺ partitioning between aragonite and fluid
818 at elevated U⁶⁺ concentration, *Geochim. Cosmochim. Acta*, 72(16), 4058–4068,
819 doi:10.1016/j.gca.2008.05.047, 2008.

820 Gabitov, R. I., Schmitt, A. K., Rosner, M., McKeegan, K. D., Gaetani, G. A., Cohen, A. L.,
821 Watson, E. B. and Harrison, T. M.: In situ $\delta^7\text{Li}$, Li/Ca, and Mg/Ca analyses of synthetic
822 aragonites, *Geochemistry, Geophys. Geosystems*, 12(3), n/a-n/a,
823 doi:10.1029/2010GC003322, 2011.

824 Gagnon, A. C., Adkins, J. F., Fernandez, D. P. and Robinson, L. F.: Sr/Ca and Mg/Ca vital
825 effects correlated with skeletal architecture in a scleractinian deep-sea coral and the role of
826 Rayleigh fractionation, *Earth Planet. Sci. Lett.*, 261(1–2), 280–295,
827 doi:10.1016/j.epsl.2007.07.013, 2007.

828 Gagnon, A. C., Adkins, J. F. and Erez, J.: Seawater transport during coral biomineralization,
829 *Earth Planet. Sci. Lett.*, 329–330, 150–161, doi:10.1016/j.epsl.2012.03.005, 2012.

830 Gordon, C. M., Carr, R. A. and Larson, R. E.: the Influence of Environmental Factors on the
831 Sodium and Manganese Content of Barnacle Shells, *Limnol. Oceanogr.*, 15(3), 461–466,

- 832 doi:10.4319/lo.1970.15.3.0461, 1970.
- 833 Hathorne, E. C., Gagnon, A., Felis, T., Adkins, J., Asami, R., Boer, W., Caillon, N., Case, D.,
834 Cobb, K. M., Douville, E., DeMenocal, P., Eisenhauer, A., Garbe-Schönberg, D., Geibert, W.,
835 Goldstein, S., Hughen, K., Inoue, M., Kawahata, H., Kölling, M., Cornec, F. L., Linsley, B. K.,
836 McGregor, H. V., Montagna, P., Nurhati, I. S., Quinn, T. M., Raddatz, J., Rebaubier, H.,
837 Robinson, L., Sadekov, A., Sherrell, R., Sinclair, D., Tudhope, A. W., Wei, G., Wong, H., Wu,
838 H. C. and You, C.-F.: Interlaboratory study for coral Sr/Ca and other element/Ca ratio
839 measurements, *Geochemistry, Geophys. Geosystems*, 14(9), 3730–3750,
840 doi:10.1002/ggge.20230, 2013.
- 841 Hauzer, H., Evans, D., Müller, W., Rosenthal, Y. and Erez, J.: Calibration of Na partitioning in
842 the calcitic foraminifer *Operculina ammonoides* under variable Ca concentration: Toward
843 reconstructing past seawater composition, *Earth Planet. Sci. Lett.*, 497, 80–91,
844 doi:10.1016/j.epsl.2018.06.004, 2018.
- 845 Haynes, W. M., Lide, D. R. and Bruno, T. J.: *CRC Handbook of chemistry and physics : a*
846 *ready-reference book of chemical and physical data.*, 2016.
- 847 Henry, L.-A. and Roberts, J. M.: *Global Biodiversity in Cold-Water Coral Reef Ecosystems, in*
848 *Marine Animal Forests*, pp. 1–21, Springer International Publishing, Cham., 2016.
- 849 Holcomb, M., Cohen, A. L., Gabitov, R. I. and Hutter, J. L.: Compositional and morphological
850 features of aragonite precipitated experimentally from seawater and biogenically by corals,
851 *Geochim. Cosmochim. Acta*, 73(14), 4166–4179, doi:10.1016/j.gca.2009.04.015, 2009.
- 852 Ip, Y. K. and Lim, A. L. L.: Are calcium and strontium transported by the same mechanism in
853 the hermatypic coral *Galaxea fascicularis*?, *J. Exp. Biol.*, 159, 507–513, 1991.
- 854 Ishikawa, M. and Ichikuni, M.: Uptake of sodium and potassium by calcite, *Chem. Geol.*,
855 42(1–4), 137–146, doi:10.1016/0009-2541(84)90010-X, 1984.
- 856 Israelson, C. and Buchardt, B.: Strontium and oxygen isotopic composition of East
857 Greenland rivers and surface waters: Implication for palaeoenvironmental interpretation,
858 *Palaeogeogr. Palaeoclimatol. Palaeoecol.*, 153(1–4), 93–104, doi:10.1016/S0031-
859 0182(99)00068-1, 1999.
- 860 Jurikova, H., Liebetrau, V., Raddatz, J., Fietzke, J., Trotter, J., Rocholl, A., Krause, S.,
861 McCulloch, M., Rüggeberg, A. and Eisenhauer, A.: Boron isotope composition of the cold-
862 water coral *Lophelia pertusa* along the Norwegian margin: Zooming into a potential pH-proxy
863 by combining bulk and high-resolution approaches, *Chem. Geol.*, #pageRange#,
864 doi:10.1016/j.chemgeo.2019.01.005, 2019.
- 865 Khani, M. H., Pahlavanzadeh, H. and Alizadeh, K.: Biosorption of strontium from aqueous
866 solution by fungus *Aspergillus terreus*, *Environ. Sci. Pollut. Res.*, 19(6), 2408–2418,
867 doi:10.1007/s11356-012-0753-z, 2012.
- 868 Kinsman, D.: Trace cations in aragonite, *Abstr. Geol. Soc. Am.*, 2, 596–597, 1970.
- 869 Kiriakoulakis, K., Fisher, E., Wolff, G. A., Freiwald, A., Grehan, A. and Roberts, J. M.: Lipids
870 and nitrogen isotopes of two deep-water corals from the North-East Atlantic: initial results
871 and implications for their nutrition, in *Cold-Water Corals and Ecosystems*, pp. 715–729,
872 Springer-Verlag, Berlin/Heidelberg., 2005.
- 873 Kiriakoulakis, K., Freiwald, A., Fisher, E. and Wolff, G. A.: Organic matter quality and supply
874 to deep-water coral/mound systems of the NW European Continental Margin, *Int. J. Earth*
875 *Sci.*, 96(1), 159–170, doi:10.1007/s00531-006-0078-6, 2007.
- 876 Kitano, Y., Okumura, M. and Idogaki, M.: Incorporation of sodium, chloride and sulfate with
877 calcium carbonate., *Geochem. J.*, 9(2), 75–84, doi:10.2343/geochemj.9.75, 1975.

878 Kunioka, D., Shirai, K., Takahata, N., Sano, Y., Toyofuku, T. and Ujiie, Y.: Microdistribution of
879 Mg/Ca, Sr/Ca, and Ba/Ca ratios in *Pulleniatina obliquiloculata* test by using a NanoSIMS:
880 Implication for the vital effect mechanism, *Geochemistry, Geophys. Geosystems*, 7(12),
881 doi:10.1029/2006GC001280, 2006.

882 Lear, C., Elderfield, H. and Wilson, P.: Cenozoic {Deep-Sea} Temperatures and Global Ice
883 Volumes from {Mg/Ca} in Benthic Foraminiferal Calcite, *Science* (80-.), 287(5451), 269–
884 272, doi:10.1126/science.287.5451.269, 2000.

885 Lewis, E. and Wallace, D. W.: R: Program developed for CO₂ system calculations
886 ORNL/CDIAC-105, Carbon Dioxide Inf. Anal. Centre Oak Ridge Natl. Lab. US Dep. Energy,
887 Oak Ridge, Tennessee, 1998.

888 Locarnini, R. A., Mishonov, A. V, Antonov, J. I., Boyer, T. P., Garcia, H. E., Baranova, O. K.,
889 Zweng, M. M., Paver, C. R., Reagan, J. R., Johnson, D. R., Hamilton, M., Seidov 1948-, D.
890 and Levitus, S.: World ocean atlas 2013. Volume 1, Temperature, edited by O. C. L. National
891 Oceanographic Data Center (U.S.) and N. E. S. United States Data, and Information
892 Service, , doi:http://doi.org/10.7289/V55X26VD, 2013.

893 López Correa, M., Montagna, P., Vendrell-Simón, B., McCulloch, M. and Taviani, M.: Stable
894 isotopes ($\delta^{18}\text{O}$ and $\delta^{13}\text{C}$), trace and minor element compositions of Recent scleractinians
895 and Last Glacial bivalves at the Santa Maria di Leuca deep-water coral province, Ionian Sea,
896 *Deep. Res. Part II Top. Stud. Oceanogr.*, 57(5–6), 471–486, doi:10.1016/j.dsr2.2009.08.016,
897 2010.

898 Lorens, R. B. and Bender, M. L.: The impact of solution chemistry on *Mytilus edulis* calcite
899 and aragonite, *Geochim. Cosmochim. Acta*, 44(9), 1265–1278, doi:10.1016/0016-
900 7037(80)90087-3, 1980.

901 Malone, P. G. and Dodd, J. R.: Temperature and salinity effects on calcification rate in
902 *Mytilus edulis* and its paleoecological implications, *Limnol. Oceanogr.*, 12(3), 432–436,
903 doi:10.4319/lo.1967.12.3.0432, 1967.

904 Marriott, C. S., Henderson, G. M., Belshaw, N. S. and Tudhope, A. W.: Temperature
905 dependence of $\delta^7\text{Li}$, $\delta^{44}\text{Ca}$ and Li/Ca during growth of calcium carbonate, *Earth Planet. Sci.*
906 *Lett.*, 222(2), 615–624, doi:10.1016/j.epsl.2004.02.031, 2004.

907 Marshall, A. T.: Calcification in hermatypic and ahermatypic corals, *Science* (80-.),
908 271(5249), 637–639, doi:10.1126/science.271.5249.637, 1996.

909 McConnaughey, T.: ^{13}C and ^{18}O isotopic disequilibrium in biological carbonates: I. Patterns,
910 *Geochim. Cosmochim. Acta*, 53(1), 151–162, doi:10.1016/0016-7037(89)90282-2, 1989.

911 McCulloch, M., Trotter, J., Montagna, P., Falter, J., Dunbar, R., Freiwald, A., Försterra, G.,
912 López Correa, M., Maier, C., Rüggeberg, A. and Taviani, M.: Resilience of cold-water
913 scleractinian corals to ocean acidification: Boron isotopic systematics of pH and saturation
914 state up-regulation, *Geochim. Cosmochim. Acta*, 87, 21–34, doi:10.1016/j.gca.2012.03.027,
915 2012.

916 van der Meer, M. T. J., Baas, M., Rijpstra, W. I. C., Marino, G., Rohling, E. J., Sinninghe
917 Damsté, J. S. and Schouten, S.: Hydrogen isotopic compositions of long-chain alkenones
918 record freshwater flooding of the Eastern Mediterranean at the onset of sapropel deposition,
919 *Earth Planet. Sci. Lett.*, 262(3–4), 594–600, doi:10.1016/j.epsl.2007.08.014, 2007.

920 Meibom, A., Cuif, J. P., Hillion, F., Constantz, B. R., Juillet-Leclerc, A., Dauphin, Y.,
921 Watanabe, T. and Dunbar, R. B.: Distribution of magnesium in coral skeleton, *Geophys. Res.*
922 *Lett.*, 31(23), 1–4, doi:10.1029/2004GL021313, 2004.

923 Mertens, K. N., Ribeiro, S., Bouimetarhan, I., Caner, H., Combourieu Nebout, N., Dale, B.,
924 De Vernal, A., Ellegaard, M., Filipova, M., Godhe, A., Goubert, E., Grøsfjeld, K., Holzwarth,

- 925 U., Kotthoff, U., Leroy, S. A. G., Londeix, L., Marret, F., Matsuoka, K., Mudie, P. J., Naudts,
 926 L., Peña-Manjarrez, J. L., Persson, A., Popescu, S. M., Pospelova, V., Sangiorgi, F., van der
 927 Meer, M. T. J., Vink, A., Zonneveld, K. A. F., Vercauteren, D., Vlassenbroeck, J. and
 928 Louwye, S.: Process length variation in cysts of a dinoflagellate, *Lingulodinium*
 929 *machaerophorum*, in surface sediments: Investigating its potential as salinity proxy, *Mar.*
 930 *Micropaleontol.*, 70(1–2), 54–69, doi:10.1016/j.marmicro.2008.10.004, 2009.
- 931 Mezger, E. M., de Nooijer, L. J., Boer, W., Brummer, G. J. A. and Reichart, G. J.: Salinity
 932 controls on Na incorporation in Red Sea planktonic foraminifera, *Paleoceanography*, 31(12),
 933 1562–1582, doi:10.1002/2016PA003052, 2016.
- 934 Mienis, F., de Stigter, H. C., White, M., Duineveld, G., de Haas, H. and van Weering, T. C.
 935 E.: Hydrodynamic controls on cold-water coral growth and carbonate-mound development at
 936 the SW and SE Rockall Trough Margin, NE Atlantic Ocean, *Deep. Res. Part I Oceanogr.*
 937 *Res. Pap.*, 54(9), 1655–1674, doi:10.1016/j.dsr.2007.05.013, 2007.
- 938 Mitsuguchi, T., Matsumoto, E., Abe, O., Uchida, T. and Isdale, P. J.: Mg/Ca thermometry in
 939 coral skeletons, *Science (80-.)*, 274(5289), 961–963, doi:10.1126/science.274.5289.961,
 940 1996.
- 941 Mitsuguchi, T., Uchida, T., Matsumoto, E., Isdale, P. J. and Kawana, T.: Variations in Mg/Ca,
 942 Na/Ca, and Sr/Ca ratios of coral skeletons with chemical treatments: implications for
 943 carbonate geochemistry, *Geochim. Cosmochim. Acta*, 65(17), 2865–2874,
 944 doi:10.1016/S0016-7037(01)00626-3, 2001.
- 945 Montagna, P., McCulloch, M., Douville, E., López Correa, M., Trotter, J., Rodolfo-Metalpa,
 946 R., Dissard, D., Ferrier-Pagès, C., Frank, N., Freiwald, A., Goldstein, S., Mazzoli, C.,
 947 Reynaud, S., Rüggeberg, A., Russo, S. and Taviani, M.: Li/Mg systematics in scleractinian
 948 corals: Calibration of the thermometer, *Geochim. Cosmochim. Acta*, 132, 288–310,
 949 doi:10.1016/j.gca.2014.02.005, 2014.
- 950 Mucci, A.: Manganese uptake during calcite precipitation from seawater: Conditions leading
 951 to the formation of a pseudokutnahorite, *Geochim. Cosmochim. Acta*, 52(7), 1859–1868,
 952 doi:10.1016/0016-7037(88)90009-9, 1988.
- 953 Mucci, A. and Morse, J.: Chemistry of low-temperature abiogenic calcites: Experimental studies
 954 on coprecipitation, stability, and fractionation, *Rev. Aquat. Sci.*, 3(2–3), 217–254, 1990.
- 955 Neulinger, S. C., Järnegren, J., Ludvigsen, M., Lochte, K. and Dullo, W. C.: Phenotype-
 956 specific bacterial communities in the cold-water coral *Lophelia pertusa* (Scleractinia) and
 957 their implications for the coral's nutrition, health, and distribution, *Appl. Environ. Microbiol.*,
 958 74(23), 7272–7285, doi:10.1128/AEM.01777-08, 2008.
- 959 Okai, T., Suzuki, A., Kawahata, H., Terashima, S. and Imai, N.: Preparation of a New
 960 Geological Survey of Japan Geochemical Reference Material: Coral JCp-1, *Geostand.*
 961 *Geoanalytical Res.*, 26(1), 95–99, doi:10.1111/j.1751-908X.2002.tb00627.x, 2002.
- 962 Okazaki, K.: SKELETON FORMATION OF SEA URCHIN LARVAE. I. EFFECT OF CA
 963 CONCENTRATION OF THE MEDIUM, *Biol. Bull.*, 110(3), 320–333, doi:10.2307/1538838,
 964 1956.
- 965 Okumura, M. and Kitano, Y.: Coprecipitation of alkali metal ions with calcium carbonate,
 966 *Geochim. Cosmochim. Acta*, 50(1), 49–58, doi:10.1016/0016-7037(86)90047-5, 1986.
- 967 Pagliarani, A., Bandiera, P., Ventrella, V., Trombetti, F., Pirini, M. and Borgatti, A. R.:
 968 Response to alkyltins of two Na⁺-dependent ATPase activities in *Tapes philippinarum* and
 969 *Mytilus galloprovincialis*, *Toxicol. Vitro.*, 20(7), 1145–1153, doi:10.1016/j.tiv.2006.02.006,
 970 2006.
- 971 Pytkowicz, R. M. and Connors, D. N.: High pressure solubility of calcium carbonate in

- 972 seawater, *Science* (80-.), 144(3620), 840–841, doi:10.1126/science.144.3620.840, 1964.
- 973 Raddatz, J., Liebetrau, V., Rüggeberg, A., Hathorne, E., Krabbenhöft, A., Eisenhauer, A.,
974 Böhm, F., Vollstaedt, H., Fietzke, J., Correa, M. L., Freiwald, A. and Dullo, W.: Stable Sr-
975 isotope , Sr / Ca , Mg / Ca , Li / Ca and Mg / Li ratios in the scleractinian cold-water coral
976 *Lophelia pertusa*, *Chem. Geol.*, 352, 143–152, doi:10.1016/j.chemgeo.2013.06.013, 2013.
- 977 Raddatz, J., Rüggeberg, A., Liebetrau, V., Foubert, A., Hathorne, E. C., Fietzke, J.,
978 Eisenhauer, A. and Dullo, W. C.: Environmental boundary conditions of cold-water coral
979 mound growth over the last 3 million years in the Porcupine Seabight, Northeast Atlantic,
980 *Deep. Res. Part II Top. Stud. Oceanogr.*, 99, 227–236, doi:10.1016/j.dsr2.2013.06.009,
981 2014a.
- 982 Raddatz, J., Rüggeberg, A., Flögel, S., Hathorne, E. C., Liebetrau, V., Eisenhauer, A. and
983 Dullo, W. C.: The influence of seawater pH on U/Ca ratios in the scleractinian cold-water
984 coral *Lophelia pertusa*, *Biogeosciences*, 11(7), 1863–1871, doi:10.5194/bg-11-1863-2014,
985 2014b.
- 986 Raddatz, J., Liebetrau, V., Trotter, J., Rüggeberg, A., Flögel, S., Dullo, W. C., Eisenhauer, A.,
987 Voigt, S. and McCulloch, M.: Environmental constraints on Holocene cold-water coral reef
988 growth off Norway: Insights from a multiproxy approach, *Paleoceanography*, 31(10), 1350–
989 1367, doi:10.1002/2016PA002974, 2016.
- 990 Ragland, P. C., Pilkey, O. H. and Blackwelder, B. W.: Diagenetic changes in the elemental
991 composition of unrecrystallized mollusk shells, *Chem. Geol.*, 25(1–2), 123–134,
992 doi:10.1016/0009-2541(79)90088-3, 1979.
- 993 Ramos, A. A., Inoue, Y. and Ohde, S.: Metal contents in *Porites* corals: Anthropogenic input
994 of river run-off into a coral reef from an urbanized area, Okinawa, *Mar. Pollut. Bull.*, 48(3–4),
995 281–294, doi:10.1016/j.marpolbul.2003.08.003, 2004.
- 996 Roberts, J. M.: *Reefs of the Deep: The Biology and Geology of Cold-Water Coral*
997 *Ecosystems*, *Science* (80-.), 312(5773), 543–547, doi:10.1126/science.1119861, 2006.
- 998 Roberts, J. M., Wheeler, A., Freiwald, A. and Cairns, S.: *Cold-Water Corals*, Cambridge
999 University Press, Cambridge., 2009.
- 1000 Robinson, L. F., Adkins, J. F., Frank, N., Gagnon, A. C., Prouty, N. G., Brendan Roark, E.
1001 and de Flierd, T. van: The geochemistry of deep-sea coral skeletons: A review of vital
1002 effects and applications for palaeoceanography, *Deep. Res. Part II Top. Stud. Oceanogr.*,
1003 99, 184–198, doi:10.1016/j.dsr2.2013.06.005, 2014.
- 1004 Roder, C., Berumen, M. L., Bouwmeester, J., Papathanassiou, E., Al-Suwailem, A. and
1005 Voolstra, C. R.: First biological measurements of deep-sea corals from the Red Sea, *Sci.*
1006 *Rep.*, 3(1), 2802, doi:10.1038/srep02802, 2013.
- 1007 Rollion-Bard, C. and Blamart, D.: SIMS method and examples of applications in coral
1008 biomineralization, *Biominer. Sourceb.*, (March), 249–261, doi:10.1201/b16621-20, 2014.
- 1009 Rollion-Bard, C. and Blamart, D.: Possible controls on Li, Na, and Mg incorporation into
1010 aragonite coral skeletons, *Chem. Geol.*, 396, 98–111, doi:10.1016/j.chemgeo.2014.12.011,
1011 2015.
- 1012 Rollion-Bard, C., Blamart, D., Cuif, J. P. and Dauphin, Y.: In situ measurements of oxygen
1013 isotopic composition in deep-sea coral, *Lophelia pertusa*: Re-examination of the current
1014 geochemical models of biomineralization, *Geochim. Cosmochim. Acta*, 74(4), 1338–1349,
1015 doi:10.1016/j.gca.2009.11.011, 2010.
- 1016 Rollion-Bard, C., Blamart, D., Trebosc, J., Tricot, G., Mussi, A. and Cuif, J. P.: Boron isotopes
1017 as pH proxy: A new look at boron speciation in deep-sea corals using ^{11}B MAS NMR and
1018 EELS, *Geochim. Cosmochim. Acta*, 75(4), 1003–1012, doi:10.1016/j.gca.2010.11.023, 2011.

- 1019 Rosenthal, Y., Field, M. P. and Sherrell, R. M.: Precise Determination of Element/Calcium
1020 Ratios in Calcareous Samples Using Sector Field Inductively Coupled Plasma Mass
1021 Spectrometry, *Anal. Chem.*, 71(15), 3248–3253, doi:10.1021/ac981410x, 1999.
- 1022 Rucker, J. B. and Valentine, J. W.: Salinity response of trace element concentration in
1023 *Crassostrea virginica*, *Nature*, 190(4781), 1099–1100, doi:10.1038/1901099a0, 1961.
- 1024 Rüggeberg, A., Flögel, S., Dullo, W. C., Hissmann, K. and Freiwald, A.: Water mass
1025 characteristics and sill dynamics in a subpolar cold-water coral reef setting at Stjærnesund,
1026 northern Norway, *Mar. Geol.*, 282(1–2), 5–12, doi:10.1016/j.margeo.2010.05.009, 2011.
- 1027 Ruiz-Hernandez, S. E., Grau-Crespo, R., Almora-Barrios, N., Wolthers, M., Ruiz-Salvador, A.
1028 R., Fernandez, N. and De Leeuw, N. H.: Mg/Ca partitioning between aqueous solution and
1029 aragonite mineral: A molecular dynamics study, *Chem. - A Eur. J.*, 18(32), 9828–9833,
1030 doi:10.1002/chem.201200966, 2012.
- 1031 Schouten, S., Ossebaar, J., Schreiber, K., Kienhuis, M. V. M., Langer, G., Benthien, A. and
1032 Bijma, J.: The effect of temperature, salinity and growth rate on the stable hydrogen isotopic
1033 composition of long chain alkenones produced by *Emiliana huxleyi* and *Gephyrocapsa*
1034 *oceanica*, *Biogeosciences*, 3(1), 113–119, doi:10.5194/bg-3-113-2006, 2006.
- 1035 Sevilgen, D. S., Venn, A. A., Hu, M. Y., Tambutté, E., de Beer, D., Planas-Bielsa, V. and
1036 Tambutté, S.: Full in vivo characterization of carbonate chemistry at the site of calcification in
1037 corals, *Sci. Adv.*, 5(1), eaau7447, doi:10.1126/sciadv.aau7447, 2019.
- 1038 Shelton, G. A. B.: *LOPHELIA pertusa* (L.): Electrical conduction and behaviour in a deep-
1039 water coral, *J. Mar. Biol. Assoc. United Kingdom*, 60(2), 517–528,
1040 doi:10.1017/S0025315400028538, 1980.
- 1041 Shirai, K., Kusakabe, M., Nakai, S., Ishii, T., Watanabe, T., Hiyagon, H. and Sano, Y.: Deep-
1042 sea coral geochemistry: Implication for the vital effect, *Chem. Geol.*, 224(4), 212–222,
1043 doi:10.1016/j.chemgeo.2005.08.009, 2005.
- 1044 Sinclair, D. J., Williams, B. and Risk, M.: A biological origin for climate signals in corals -
1045 Trace element “vital effects” are ubiquitous in Scleractinian coral skeletons, *Geophys. Res.*
1046 *Lett.*, 33(17), 1–5, doi:10.1029/2006GL027183, 2006.
- 1047 Sizer, I. W.: Effects of temperature on enzyme kinetics, in *Advances in Enzymology and*
1048 *Related Areas of Molecular Biology*, pp. 35–62, Wiley-Blackwell., 2006.
- 1049 Stolarski, J.: Three-dimensional micro- and nanostructural characteristics of the scleractinian
1050 coral skeleton: A biocalcification proxy, *Acta Palaeontol. Pol.*, 48(4), 497–530, doi:Available
1051 from: <http://www.app.pan.pl/article/item/app48-497.html>., 2003.
- 1052 Swart, P. K.: The strontium, magnesium and sodium composition of recent scleractinian coral
1053 skeletons as standards for palaeoenvironmental analysis, *Palaeogeogr. Palaeoclimatol.*
1054 *Palaeoecol.*, 34(C), 115–136, doi:10.1016/0031-0182(81)90060-2, 1981.
- 1055 Tambutté, E., Allemand, D., Zoccola, D., Meibom, A., Lotto, S., Caminiti, N. and Tambutté,
1056 S.: Observations of the tissue-skeleton interface in the scleractinian coral *Stylophora*
1057 *pistillata*, *Coral Reefs*, 26(3), 517–529, doi:10.1007/s00338-007-0263-5, 2007.
- 1058 Tambutté, S., Holcomb, M., Ferrier-Pagès, C., Reynaud, S., Tambutté, É., Zoccola, D. and
1059 Allemand, D.: Coral biomineralization: From the gene to the environment, *J. Exp. Mar. Bio.*
1060 *Ecol.*, 408(1–2), 58–78, doi:10.1016/j.jembe.2011.07.026, 2011.
- 1061 Taviani, M., Remia, A., Corselli, C., Freiwald, A., Malinverno, E., Mastrototaro, F., Savini, A.
1062 and Tursi, A.: First geo-marine survey of living cold-water *Lophelia* reefs in the Ionian Sea
1063 (Mediterranean basin), *Facies*, 50(3–4), 409–417, doi:10.1007/s10347-004-0039-0, 2005.
- 1064 Trivedi, B. and Danforth, W. H.: Effect of pH on the kinetics of frog muscle

- 1065 phosphofructokinase., *J. Biol. Chem.*, 241(17), 4110–4112, doi:10.2196/jmir.1752, 1966.
- 1066 Turekian, K. K., Steele, J. H. and Thorpe, S. A.: *Marine Chemistry & Geochemistry A*
1067 *DERIVATIVE OF ENCYCLOPEDIA OF OCEAN SCIENCES.*, 2010.
- 1068 de Villiers, S., Shen, G. T. and Nelson, B. K.: The Sr/Ca-temperature relationship in coralline
1069 aragonite: Influence of variability in (Sr/Ca)Seawater and skeletal growth parameters,
1070 *Geochim. Cosmochim. Acta*, 58(1), 197–208, doi:10.1016/0016-7037(94)90457-X, 1994.
- 1071 Wang, K., Villalobo, A. and Roufogalis, B.: The plasma membrane calcium pump: a
1072 multiregulated transporter, *Trends Cell Biol.*, 2(February), 46–52 [online] Available from:
1073 <http://www.ncbi.nlm.nih.gov/pubmed/14731526> (Accessed 22 August 2018), 1992.
- 1074 Wang, W. X. and Fisher, N. S.: Effects of calcium and metabolic inhibitors on trace element
1075 uptake in two marine bivalves, *J. Exp. Mar. Bio. Ecol.*, 236(1), 149–164, doi:10.1016/S0022-
1076 0981(98)00195-6, 1999.
- 1077 Watson, E. B.: WATSON - surface enrichment and trace-element uptake during crystal
1078 growth, , 60(24), 5013–5020, 1996.
- 1079 Weldeab, S., Lea, D. W., Schneider, R. R. and Andersen, N.: Centennial scale climate
1080 instabilities in a wet early Holocene West African monsoon, *Geophys. Res. Lett.*, 34(24), 1–
1081 6, doi:10.1029/2007GL031898, 2007.
- 1082 White, A. F.: Sodium and potassium coprecipitation in aragonite, *Geochim. Cosmochim.*
1083 *Acta*, 41(5), 613–625, doi:10.1016/0016-7037(77)90301-5, 1977.
- 1084 Wit, J. C., De Nooijer, L. J., Wolthers, M. and Reichart, G. J.: A novel salinity proxy based on
1085 na incorporation into foraminiferal calcite, *Biogeosciences*, 10(10), 6375–6387,
1086 doi:10.5194/bg-10-6375-2013, 2013.
- 1087 Yamazato, K.: Calcification in a solitary coral, *Fungia scutaria* Lamarck in relation to
1088 environmental factors, 1966.
- 1089 Yoshimura, T., Tamemori, Y., Suzuki, A., Kawahata, H., Iwasaki, N., Hasegawa, H., Nguyen,
1090 L. T., Kuroyanagi, A., Yamazaki, T., Kuroda, J. and Ohkouchi, N.: Altrivalent substitution of
1091 sodium for calcium in biogenic calcite and aragonite, *Geochim. Cosmochim. Acta*, 202, 21–
1092 38, doi:10.1016/j.gca.2016.12.003, 2017.
- 1093 Zeebe, R. E. and Wolf-Gladrow, D. A.: CO₂ in seawater : equilibrium, kinetics, isotopes.
1094 [online] Available from: <http://epic.awi.de/4276/> (Accessed 22 August 2018), 2001.
- 1095 Zonneveld, K. A. F., P. Hoek, R., Brinkhuis, H. and Helmut Willems: Geographical
1096 distributions of organic-walled dinoflagellate cysts in surficial sediments of the Benguela
1097 upwelling region and their relationship to upper ocean conditions, *Prog. Oceanogr.*, 48(1),
1098 25–72, doi:10.1016/S0079-6611(00)00047-1, 2001.
- 1099 Zweng, M. M., Reagan, J. R., Antonov, J. I., Locarnini, R. A., Mishonov, A. V, Boyer, T. P.,
1100 Garcia, H. E., Baranova, O. K., Johnson, D. R., Seidov 1948-, D., Biddle, M. M. and Levitus,
1101 S.: *World ocean atlas 2013. Volume 2, Salinity*, edited by O. C. L. National Oceanographic
1102 Data Center (U.S.) and N. E. S. United States Data, and Information Service, ,
1103 doi:<http://doi.org/10.7289/V5251G4D>, 2013.
- 1104 Zweng, M. M., Reagan, J. R., Antonov, J. I., Locarnini, R. A., Mishonov, A. V, Boyer, T. P.,
1105 Garcia, H. E., Baranova, O. K., Johnson, D. R., Seidov 1948-, D., Biddle, M. M. and Levitus,
1106 S.: *World ocean atlas 2013. Volume 2, Salinity*, edited by O. C. L. National Oceanographic
1107 Data Center (U.S.) and N. E. S. United States Data, and Information Service, ,
1108 doi:<http://doi.org/10.7289/V5251G4D>, 2013.
- 1109